Available online at www.sciencedirect.com
SCIENCE DIRECT®
ELSEVIER
International Journal of Solids and Structures 42 (2005) 5795–5820
INTERNATIONAL JOURNAL OF SOLIDS and STRUCTURES
www.elsevier.com/locate/ijsolstr

Evaluation of multi-modes for finite-element models: systems tuned into 1:2 internal resonance

O.G.P. Baracho Neto, C.E.N. Mazzilli *

Laboratório de Mecânica Computacional, Departamento de Engenharia de Estruturas e Fundações, Escola Politécnica da Universidade de São Paulo, Caixa Postal 61548—CEP 05424-970 São Paulo, Brazil

Received 18 February 2005
Available online 14 April 2005

Abstract

A non-linear multi-mode of vibration arises from the coupling of two or more normal modes of a non-linear system under free-vibration. The ensuing motion takes place on a $2M$-dimensional invariant manifold in the phase space of the system, M being the number of coupled linear modes; the manifold contains a stable equilibrium point of interest, and at that point is tangent to the $2M$-dimensional eigenspace of the system linearised about that equilibrium point, which characterises the corresponding M linear modes. On this manifold, M pairs of state variables govern the dynamics of the system; that is, the system behaves like an M-degree-of-freedom oscillator. Non-linear multi-modes may therefore come about when the system exhibits non-linear coupling among generalised co-ordinates. That is the case, for instance, of internal resonance of the 1:2 or 1:3 types, for systems with quadratic or cubic non-linearities, respectively, in which a four-dimensional manifold should be determined. Evaluation of non-linear multi-modes poses huge computational challenges, which is the explanation for very limited reports on the subject in the literature so far. The authors developed a procedure to determine the non-linear multi-modes for finite-element models of plane frames, using the method of multiple scales. This paper refers to the case of quadratic non-linearities. The results obtained by the proposed technique are in good agreement with those coming out from direct integration of the equations of motion in the time domain and also with those few available in the literature.

Keywords: Non-linear dynamics; Non-linear modes; Non-linear multi-modes; Quadratic non-linearities; Finite-element model; Reduction technique

* Corresponding author. Tel.: +55 1130 915232; fax: +55 1130 915181.
E-mail address: cenmazzi@usp.br (C.E.N. Mazzilli).

0020-7683/$ - see front matter © 2005 Elsevier Ltd. All rights reserved.
doi:10.1016/j.ijsolstr.2005.03.026

1. Introduction

According to Boivin et al. (1994), Boivin et al. (1995a) and Boivin et al. (1995b), non-linear multi-modes of vibration can be understood as an extension of the non-linear normal modes, in the case two or more of them interact. Such interactions are stronger in presence of internal resonance. The ensuing free vibration motion takes place in an invariant manifold embedded in the phase space, whose dimension is twice the number of the normal modes which interact. This manifold contains a stable equilibrium point, and is tangent there to the sub-eigenspace of the linearised system, which characterises the corresponding linear modes. The multi-mode can be locally described by a linear combination of the linear modes. On this manifold, the system behaves like an M-degree-of-freedom oscillator, where M is the number of coupled normal modes.

Both non-linear normal modes and multi-modes may be efficient projection functions to be used in the reduction of degrees of freedom of non-linear systems, according to Mazzilli et al. (2001).

The authors developed a technique based on the method of multiple scales to evaluate the non-linear multi-modes of discrete systems whose equations of motion are of the form of (1). Such a technique is an extension of the procedure already proposed by them with success to the evaluation of non-linear normal modes, see Mazzilli and Baracho Neto (2002).

For simplicity and conciseness in the presentation, this paper will consider only systems in which the quadratic non-linearities are the important ones, such that there are only two coupled normal modes in internal resonance, their linear frequencies being in the 1:2 ratio. For systems with cubic non-linearities and internal resonance of the 1:3 type, reference is made to Baracho Neto and Mazzilli (2005).

Suppose the equations of motion for a non-linear system with n degrees of freedom are of the form (1), which is sufficiently general to accommodate not only systems that are naturally discrete, but also those discretised by the finite-element method. That is, for instance, the case of planar frames, see Mazzilli and Baracho Neto (2002).

$$M_{rs}\ddot{p}_s + D_{rs}\dot{p}_s + U_{,r} = \mathscr{F}_r \tag{1}$$

$$\begin{aligned} M_{rs} &= {}^0M_{rs} + {}^1M^i_{rs}p_i + {}^2M^{ij}_{rs}p_ip_j \\ D_{rs} &= {}^0D_{rs} + {}^1D^i_{rs}\dot{p}_i + {}^2D^{ij}_{rs}\dot{p}_ip_j \\ U_{,r} &= {}^0K_{rs}p_s + {}^1K^i_{rs}p_ip_s + {}^2K^{ij}_{rs}p_ip_jp_s \end{aligned} \tag{2}$$

$[M]$ and $[D]$ are, respectively, the matrices of mass and equivalent viscous damping, and $\{U\}$ and $\{F\}$ are, respectively, the elastic force and the applied load vectors. This latter one is usually null in modal analysis, unless vibration about the deformed equilibrium configuration is being considered, in which case it is a static load vector. The generalised co-ordinates, velocities and accelerations are written as p_i, $\dot{p}_i$ and $\ddot{p}_i$. Einstein's notation is being used throughout the text, so that repeated indices mean summation from 1 to n, unless otherwise stated. Note that system (1) comprises both quadratic and cubic non-linearities, although, in the present study, only the quadratic non-linearities are assumed to be the important ones.

2. Non-linear multi-modes for 1:2 internal resonance: time response

Non-linear multi-modes of systems with quadratic non-linearities tuned into 1:2 internal resonance are now sought with the help of the method of multiple scales. The output will be the time response of each generalised co-ordinate in the form of an asymptotic expansion of a small positive non-dimensional perturbation parameter ε. Note that the real time t is replaced by several time scales T_k, as defined below.

$$
\begin{aligned}
T_k &= \varepsilon^k t; \quad D_i^n = \frac{\mathrm{d}^n}{\mathrm{d}T_i^n} \\
p_i(t) &= p_{i0} + \varepsilon p_{i1}(T_0, T_1, \ldots) + \varepsilon^2 p_{i2}(T_0, T_1, \ldots) + \varepsilon^3 p_{i3}(T_0, T_1, \ldots) + \cdots \\
\frac{\mathrm{d}}{\mathrm{d}t} &= D_0 + \varepsilon D_1 + \varepsilon^2 D_2 + \cdots \\
\frac{\mathrm{d}^2}{\mathrm{d}t^2} &= D_0^2 + 2\varepsilon D_0 D_1 + \varepsilon^2 (2D_0 D_2 + D_1^2) + \cdots
\end{aligned}
\tag{3}
$$

Here, p_{i0} refers to the static equilibrium configuration. After consideration of (2) and (3) in (1), as usual in the method of multiple scales, the equation of motion will be written as

$$
\begin{aligned}
&{}^0M_{rs}\left\{\left[D_0^2 + 2\varepsilon D_0 D_1 + \varepsilon^2\left(2D_0 D_2 + D_1^2\right) + \cdots\right]\left(p_{s0} + \varepsilon p_{s1} + \varepsilon^2 p_{s2} + \varepsilon^3 p_{s3} + \cdots\right)\right\} \\
&\quad + {}^0D_{rs}\left[\left(D_0 + \varepsilon D_1 + \varepsilon^2 D_2 + \cdots\right)\left(p_{s0} + \varepsilon p_{s1} + \varepsilon^2 p_{s2} + \varepsilon^3 p_{s3} + \cdots\right)\right] \\
&\quad + {}^0K_{rs}\left(p_{s0} + \varepsilon p_{s1} + \varepsilon^2 p_{s2} + \varepsilon^3 p_{s3} + \cdots\right) + {}^1M_{rs}^i\left(p_{i0} + \varepsilon p_{i1} + \varepsilon^2 p_{i2} + \varepsilon^3 p_{i3} + \cdots\right) \\
&\quad \times \left\{\left[D_0^2 + 2\varepsilon D_0 D_1 + \varepsilon^2\left(2D_0 D_2 + D_1^2\right) + \cdots\right]\left(p_{s0} + \varepsilon p_{s1} + \varepsilon^2 p_{s2} + \varepsilon^3 p_{s3} + \cdots\right)\right\} \\
&\quad + {}^1D_{rs}^i\left[\left(D_0 + \varepsilon D_1 + \varepsilon^2 D_2 + \cdots\right)\left(p_{s0} + \varepsilon p_{i1} + \varepsilon^2 p_{i2} + \varepsilon^3 p_{i3} + \cdots\right)\right] \\
&\quad \times \left[\left(D_0 + \varepsilon D_1 + \varepsilon^2 D_2 + \cdots\right)\left(p_{s0} + \varepsilon p_{s1} + \varepsilon^2 p_{s2} + \varepsilon^3 p_{s3} + \cdots\right)\right] \\
&\quad + {}^1K_{rs}^i\left(p_{i0} + \varepsilon p_{i1} + \varepsilon^2 p_{i2} + \varepsilon^3 p_{i3} + \cdots\right)\left(p_{s0} + \varepsilon p_{s1} + \varepsilon^2 p_{s2} + \varepsilon^3 p_{s3} + \cdots\right) \\
&\quad + {}^2M_{rs}^{ij}\left(p_{i0} + \varepsilon p_{i1} + \varepsilon^2 p_{i2} + \varepsilon^3 p_{i3} + \cdots\right)\left(p_{j0} + \varepsilon p_{j1} + \varepsilon^2 p_{j2} + \varepsilon^3 p_{j3} + \cdots\right) \\
&\quad \times \left\{\left[D_0^2 + 2\varepsilon D_0 D_1 + \varepsilon^2\left(2D_0 D_2 + D_1^2\right) + \cdots\right]\left(p_{s0} + \varepsilon p_{s1} + \varepsilon^2 p_{s2} + \varepsilon^3 p_{s3} + \cdots\right)\right\} \\
&\quad + {}^2D_{rs}^{ij}\left[\left(D_0 + \varepsilon D_1 + \varepsilon^2 D_2 + \cdots\right)\left(p_{i0} + \varepsilon p_{i1} + \varepsilon^2 p_{i2} + \varepsilon^3 p_{i3} + \cdots\right)\right] \\
&\quad \times \left(p_{j0} + \varepsilon p_{j1} + \varepsilon^2 p_{j2} + \varepsilon^3 p_{j3} + \cdots\right) \times \left[\left(D_0 + \varepsilon D_1 + \varepsilon^2 D_2 + \cdots\right)\left(p_{s0} + \varepsilon p_{s1} + \varepsilon^2 p_{s2} + \varepsilon^3 p_{s3} + \cdots\right)\right] \\
&\quad + {}^2K_{rs}^{ij}\left(p_{i0} + \varepsilon p_{i1} + \varepsilon^2 p_{i2} + \varepsilon^3 p_{i3} + \cdots\right)\left(p_{j0} + \varepsilon p_{j1} + \varepsilon^2 p_{j2} + \varepsilon^3 p_{j3} + \cdots\right) \\
&\quad \times \left(p_{s0} + \varepsilon p_{s1} + \varepsilon^2 p_{s2} + \varepsilon^3 p_{s3} + \cdots\right) \\
&\quad = \mathscr{F}_r
\end{aligned}
\tag{4}
$$

Obviously, for static reasons, the following relation must hold:

$$
{}^0K_{rs}p_{s0} + {}^1K_{rs}^i p_{i0}p_{s0} + {}^2K_{rs}^{ij} p_{i0}p_{j0}p_{s0} + \cdots = \mathscr{F}_r \tag{5}
$$

2.1. Equations of order ε

If only terms of order ε are retained in (4), the free vibration problem of systems linearised about the equilibrium configuration will appear

$$
{}^0M_{rs}^* D_0^2 p_{s1} + {}^0D_{rs}^* D_0 p_{s1} + {}^0K_{rs}^* p_{s1} = 0 \tag{6}
$$

where

$$
\begin{aligned}
{}^0M_{rs}^* &= {}^0M_{rs} + {}^1M_{rs}^i p_{i0} + {}^2M_{rs}^{ij} p_{i0}p_{j0} \\
{}^0D_{rs}^* &= {}^0D_{rs} \\
{}^0K_{rs}^* &= {}^0K_{rs} + \left({}^1K_{rs}^i + {}^1K_{ri}^s\right)p_{i0} + \left({}^2K_{rs}^{ij} + {}^2K_{rj}^{is} + {}^2K_{ri}^{sj}\right)p_{i0}p_{j0}
\end{aligned}
\tag{7}
$$

are respectively the mass, damping and stiffness coefficients evaluated at the equilibrium configuration. Solution of (6) is simply

$$p_{s1} = A_{s1}\mathrm{e}^{\Psi T_0}; \quad A_{s1} = A_{s1}(T_1, T_2, \ldots) \tag{8}$$

which, taken into account in (6), will lead to

$$\left(\Psi^2 {}^0M^*_{rs} + \Psi^0 D^*_{rs} + {}^0K^*_{rs}\right)A_{s1} = 0 \quad \forall r,s = 1 \text{ to } n. \tag{9}$$

This is the classic damped eigenvalue problem, for which the solvability condition is the characteristic equation:

$$\det\left(\Psi^2\left[{}^0M^*\right] + \Psi\left[{}^0D^*\right] + \left[{}^0K^*\right]\right) = 0. \tag{10}$$

The case of sub-critical damping of order $\mathrm{O}(\varepsilon)$ is here assumed, so the roots of (10) are complex

$$\Psi_u = \alpha_u + \mathrm{i}\beta_u; \quad u = 1 \text{ to } n \tag{11}$$

A convenient amplitude A^u_{v1}—corresponding to the uth mode contribution to the non-null generalised coordinate p_v—is used to normalise the remaining modal amplitudes and define the corresponding modal eigenvectors

$$\frac{A^u_{s1}}{A^u_{v1}} = \phi^u_s \Rightarrow A^u_{s1} = \phi^u_s A^u_{v1} = \left(\gamma^u_s + \mathrm{i}\delta^u_s\right)A^u_{v1}; \quad \begin{matrix} u,v,s = 1 \text{ to } n \\ \text{no sum in } u \end{matrix} \tag{12}$$

Without the risk of ambiguity, a lighter notation can be used for the modal amplitudes

$$\begin{aligned} A^u_{v1} &= A^u_1 \\ A^u_{s1} &= \phi^u_s A^u_1 = \left(\gamma^u_s + \mathrm{i}\delta^u_s\right)A^u_1; \quad \text{no sum in } u \end{aligned} \tag{13}$$

To the two resonating modes will be assigned indices I and II, respectively to those of smaller and larger frequency, so that the time response, to the order of ε, of a free vibration motion which contains solely contributions from these two modes can be written as:

$$p_{s1} = A^{\mathrm{I}}_{s1}\mathrm{e}^{\Psi_{\mathrm{I}}T_0} + A^{\mathrm{II}}_{s1}\mathrm{e}^{\Psi_{\mathrm{II}}T_0} + \text{c.c.} = \phi^{\mathrm{I}}_s A^{\mathrm{I}}_1\mathrm{e}^{\Psi_{\mathrm{I}}T_0} + \phi^{\mathrm{II}}_s A^{\mathrm{II}}_1\mathrm{e}^{\Psi_{\mathrm{II}}T_0} + \text{c.c.} \tag{14}$$

Note that (14) indicates that locally the motion takes place in the invariant manifold associated to this multi-mode, i.e. the invariant manifold is tangent to the sub-eigenspace of modes I and II.

2.2. Equations of order ε^2

Terms of order ε^2 are now retained in (4):

$$\begin{aligned} {}^0M^*_{rs}D_0^2 p_{s2} + {}^0D^*_{rs}D_0 p_{s2} + {}^0K^*_{rs}p_{s2} = &-2\left({}^0M_{rs} + {}^1M^i_{rs}p_{i0} + {}^2M^{ij}_{rs}p_{i0}p_{j0}\right)D_0D_1p_{s1} - {}^0D_{rs}D_1p_{s1} \\ &- \left({}^1M^i_{rs}p_{i1} + {}^2M^{ij}_{rs}p_{j0}p_{i1} + {}^2M^{ji}_{rs}p_{j0}p_{i1}\right)D_0^2p_{s1} \\ &- \left({}^1D^i_{rs} + {}^2D^{ij}_{rs}p_{j0}\right)\left(D_0p_{i1}D_0p_{s1}\right) \\ &- \left({}^1K^i_{rs}p_{i1} + {}^2K^{ij}_{rs}p_{j0}p_{i1} + {}^2K^{ji}_{rs}p_{j0}p_{i1} + {}^2K^{si}_{rj}p_{j0}p_{i1}\right)p_{s1}. \end{aligned} \tag{15}$$

Consider the following auxiliary expressions, which take into account the 1:2 internal resonance:

$$\begin{aligned} &\Psi_{\mathrm{I}} + \overline{\Psi}_{\mathrm{I}} = 2\alpha_{\mathrm{I}} \\ &\Psi_{\mathrm{II}} + \overline{\Psi}_{\mathrm{II}} = 2\alpha_{\mathrm{II}} \\ &\Psi_{\mathrm{II}} - 2\Psi_{\mathrm{I}} = \Delta\Psi \\ &\Psi_{\mathrm{II}} + \overline{\Psi}_{\mathrm{I}} = \Psi_{\mathrm{I}} + \alpha_{\mathrm{II}} + \mathrm{i}\Delta\beta \end{aligned} \tag{16}$$

where

$$\begin{aligned}\Delta\Psi &= \Delta\alpha + \mathrm{i}\Delta\beta\\ \Delta\alpha &= \alpha_{\mathrm{II}} - 2\alpha_{\mathrm{I}}\\ \Delta\beta &= \beta_{\mathrm{II}} - 2\beta_{\mathrm{I}}.\end{aligned} \tag{17}$$

It is assumed that the difference between Ψ_{II} and $2\Psi_{\mathrm{I}}$ is a small complex number $\Delta\Psi$. This is a reasonable assumption provided the linear frequencies are nearly in the 1:2 ratio, i.e. $\beta_{\mathrm{II}} \cong 2\beta_{\mathrm{I}}$. It is therefore assumed that $\Delta\beta = \mathrm{O}(\varepsilon)$, and the damping is small and sub-critical for both modes, so that $\Delta\alpha = \mathrm{O}(\varepsilon)$. Next, (14) and (16) are considered in (15) to justify that the order ε^2 correction to the time response should be of the form

$$p_{s2} = A^{\mathrm{I}}_{s2}\mathrm{e}^{\Psi_{\mathrm{I}}T_0} + A^{\mathrm{II}}_{s2}\mathrm{e}^{\Psi_{\mathrm{II}}T_0} + B^{\mathrm{II}}_{s2}\mathrm{e}^{2\Psi_{\mathrm{II}}T_0} + C_{s2}\mathrm{e}^{(\Psi_{\mathrm{I}}+\Psi_{\mathrm{II}})T_0} + F^{\mathrm{I}}_{s2}\mathrm{e}^{2\alpha_{\mathrm{I}}T_0} + F^{\mathrm{II}}_{s2}\mathrm{e}^{2\alpha_{\mathrm{II}}T_0} + \mathrm{c.c.} \tag{18}$$

The coefficients of (18) can be determined once (14) and (18) are taken into (15) and each frequency component is studied separately.

2.2.1. Terms in $e^{\Psi_I T_0}$

$$\begin{aligned}&\left(\Psi_{\mathrm{I}}^{2\,0}M^*_{rs} + \Psi_{\mathrm{I}}{}^{0}D^*_{rs} + {}^{0}K^*_{rs}\right)A^{\mathrm{I}}_{s2}\\ &\quad= -2\Psi_{\mathrm{I}}\phi^{\mathrm{I}}_s\left[\left({}^{0}M_{rs} + {}^{1}M^i_{rs}p_{i0} + {}^{2}M^{ij}_{rs}p_{i0}p_{j0}\right)\right]D_1A^{\mathrm{I}}_1 - \phi^{\mathrm{I}0}_s D_{rs}D_1A^{\mathrm{I}}_1\\ &\qquad- \left(\Psi^2_{\mathrm{II}}\bar{\phi}^{\mathrm{I}}_i\phi^{\mathrm{II}}_s + \overline{\Psi}^2_{\mathrm{I}}\bar{\phi}^{\mathrm{I}}_s\phi^{\mathrm{II}}_i\right)\left({}^{1}M^i_{rs} + {}^{2}M^{ij}_{rs}p_{j0} + {}^{2}M^{ji}_{rs}p_{j0}\right)\bar{A}^{\mathrm{I}}_1A^{\mathrm{II}}_1\exp\left((\alpha_{\mathrm{II}} + \mathrm{i}\Delta\beta)T_0\right)\\ &\qquad- \overline{\Psi}_{\mathrm{I}}\Psi_{\mathrm{II}}\left(\bar{\phi}^{\mathrm{I}}_i\phi^{\mathrm{II}}_s + \bar{\phi}^{\mathrm{I}}_s\phi^{\mathrm{II}}_i\right)\left({}^{1}D^i_{rs} + {}^{2}D^{ij}_{rs}p_{j0}\right)\bar{A}^{\mathrm{I}}_1A^{\mathrm{II}}_1\exp\left((\alpha_{\mathrm{II}} + \mathrm{i}\Delta\beta)T_0\right)\\ &\qquad- \left(\bar{\phi}^{\mathrm{I}}_i\phi^{\mathrm{II}}_s + \bar{\phi}^{\mathrm{I}}_s\phi^{\mathrm{II}}_i\right){}^{1}K^i_{rs}\bar{A}^{\mathrm{I}}_1A^{\mathrm{II}}_1\exp\left((\alpha_{\mathrm{II}} + \mathrm{i}\Delta\beta)T_0\right)\\ &\qquad- \left(\bar{\phi}^{\mathrm{I}}_i\phi^{\mathrm{II}}_s + \bar{\phi}^{\mathrm{I}}_s\phi^{\mathrm{II}}_i\right)\left({}^{2}K^{ij}_{rs}p_{j0} + {}^{2}K^{ji}_{rs}p_{j0} + {}^{2}K^{si}_{rj}p_{j0}\right)\bar{A}^{\mathrm{I}}_1A^{\mathrm{II}}_1\exp\left((\alpha_{\mathrm{II}} + \mathrm{i}\Delta\beta)T_0\right)\end{aligned} \tag{19}$$

It should be recalled that (10) implies that the matrix $[{}^{0}S] = \Psi^2[{}^{0}M^*] + \Psi[{}^{0}D^*] + [{}^{0}K^*]$, that appears on the left-hand side of (19), must be singular. Hence, for (19) to have solution, it is necessary that the determinant of the matrix obtained by the substitution of any column of $[{}^{0}S]$ by the vector of terms on the right-hand side of (19) be null, according to Cramer's rule. This is precisely the solvability condition for the ε^2 terms associated to the eigenvalue Ψ_{I}. Such an imposition will lead to a differential equation of the form:

$$(a_1 + \mathrm{i}b_1)D_1A^{\mathrm{I}}_1 + (c_1 + \mathrm{i}d_1)\bar{A}^{\mathrm{I}}_1A^{\mathrm{II}}_1\exp\left(\frac{(\alpha_{\mathrm{II}} + \mathrm{i}\Delta\beta)}{\varepsilon}T_1\right) = 0 \tag{20}$$

where a_1, b_1, c_1 and d_1 are real numbers.

2.2.2. Terms in $e^{\Psi_{II} T_0}$

$$\begin{aligned}&\left(\Psi_{\mathrm{II}}^{2\,0}M^*_{rs} + \Psi_{\mathrm{II}}{}^{0}D^*_{rs} + {}^{0}K^*_{rs}\right)A^{\mathrm{II}}_{s2}\\ &\quad= -2\Psi_{\mathrm{II}}\phi^{\mathrm{II}}_s\left[\left({}^{0}M_{rs} + {}^{1}M^i_{rs}p_{i0} + {}^{2}M^{ij}_{rs}p_{i0}p_{j0}\right)\right]D_1A^{\mathrm{II}}_1 - \phi^{\mathrm{II}0}_s D_{rs}D_1A^{\mathrm{II}}_1\\ &\qquad- \Psi^2_{\mathrm{I}}\phi^{\mathrm{I}}_i\phi^{\mathrm{I}}_s\left({}^{1}M^i_{rs} + {}^{2}M^{ij}_{rs}p_{j0} + {}^{2}M^{ji}_{rs}p_{j0}\right)\left(A^{\mathrm{I}}_1\right)^2\exp(-\Delta\Psi T_0)\\ &\qquad- \Psi^2_{\mathrm{I}}\phi^{\mathrm{I}}_i\phi^{\mathrm{I}}_s\left({}^{1}D^i_{rs} + {}^{2}D^{ij}_{rs}p_{j0}\right)\left(A^{\mathrm{I}}_1\right)^2\exp\left(-\Delta\Psi T_0\right)\\ &\qquad- \phi^{\mathrm{I}}_i\phi^{\mathrm{I}}_s\left({}^{1}K^i_{rs} + {}^{2}K^{ij}_{rs}p_{j0} + {}^{2}K^{ji}_{rs}p_{j0} + {}^{2}K^{si}_{rj}p_{j0}\right)\left(A^{\mathrm{I}}_1\right)^2\exp(-\Delta\Psi T_0)\end{aligned} \tag{21}$$

The reasoning for the ε^2 terms associated to the eigenvalue Ψ_{I} applies likewise to the solvability condition associated to the eigenvalue Ψ_{II}. Such an imposition will lead to a differential equation of the form

$$(a_2 + \mathrm{i}b_2)D_1A_1^{\mathrm{II}} + (c_2 + \mathrm{i}d_2)\left(A_1^{\mathrm{I}}\right)^2 \exp\left(-\frac{\Delta\Psi}{\varepsilon}T_1\right) = 0 \tag{22}$$

where a_2, b_2, c_2 and d_2 are real numbers.

2.2.3. Synthesis for terms in $e^{\Psi_I T_0}$ and $e^{\Psi_{II} T_0}$

The system of non-linear differential equations given by (21) and (22) has as unknowns the complex modal amplitudes A_1^{I} and A_1^{II}. The solution can be searched in the form

$$\begin{aligned} A_1^{\mathrm{I}} &= \frac{1}{2}a_{\mathrm{I}}\exp(\mathrm{i}\theta_{\mathrm{I}}) \\ A_1^{\mathrm{II}} &= \frac{1}{2}a_{\mathrm{II}}\exp(\mathrm{i}\theta_{\mathrm{II}}) \end{aligned} \tag{23}$$

where a_{I}, a_{II}, θ_{I}, and θ_{II} are real numbers. The system (21) and (22) is then replaced by the system of four first-order non-linear differential equations in the aforementioned real unknowns, with respect to the time scale T_1

$$\begin{aligned} D_1a_{\mathrm{I}} &= -\frac{a_{\mathrm{I}}a_{\mathrm{II}}\exp\left(\frac{\gamma_{\mathrm{II}}}{\varepsilon}T_1\right)}{2\left[(a_1)^2 + (b_1)^2\right]}\left[(a_1c_1 + b_1d_1)\cos\gamma_1 + (b_1c_1 - a_1d_1)\,\mathrm{sen}\,\gamma_1\right] \\ D_1a_{\mathrm{II}} &= -\frac{(a_{\mathrm{I}})^2\exp\left(-\frac{\Delta\alpha}{\varepsilon}T_1\right)}{2\left[(a_2)^2 + (b_2)^2\right]}\left[(a_2c_2 + b_2d_2)\cos\gamma_1 - (b_2c_2 - a_2d_2)\,\mathrm{sen}\,\gamma_1\right] \\ D_1\theta_{\mathrm{I}} &= \frac{a_{\mathrm{II}}\exp\left(\frac{\gamma_{\mathrm{II}}}{\varepsilon}T_1\right)}{2\left[(a_1)^2 + (b_1)^2\right]}\left[(b_1c_1 - a_1d_1)\cos\gamma_1 - (a_1c_1 - b_1d_1)\,\mathrm{sen}\,\gamma_1\right] \\ D_1\theta_{\mathrm{II}} &= \frac{(a_{\mathrm{I}})^2\exp\left(-\frac{\Delta\alpha}{\varepsilon}T_1\right)}{2a_{\mathrm{II}}\left[(a_2)^2 + (b_2)^2\right]}\left[(b_2c_2 - a_2d_2)\cos\gamma_1 + (a_2c_2 + b_2d_2)\,\mathrm{sen}\,\gamma_1\right] \end{aligned} \tag{24}$$

with

$$\gamma_1 = \frac{\Delta\beta}{\varepsilon}T_1 + \theta_{\mathrm{II}} - 2\theta_{\mathrm{I}} = \Delta\beta t + \theta_{\mathrm{II}} - 2\theta_{\mathrm{I}}. \tag{25}$$

Such a system does not have closed-form solution, but can be integrated numerically. The authors have implemented a routine to integrate the system (24), using a Runge–Kutta algorithm within a symbolic mathematics package. For details, refer to Baracho Neto (2003).

2.2.4. Terms in $e^{2\Psi_{II} T_0}$

$$\begin{aligned} \left(4\Psi_{\mathrm{II}}^2\,{}^0M_{rs}^* + 2\Psi_{\mathrm{II}}\,{}^0D_{rs}^* + {}^0K_{rs}^*\right)B_{s2}^{\mathrm{II}} = &-\Psi_{\mathrm{II}}^2\,{}^1M_{rs}^i\phi_i^{\mathrm{II}}\phi_s^{\mathrm{II}}\left(A_1^{\mathrm{II}}\right)^2 - \Psi_{\mathrm{II}}^2\left({}^2M_{rs}^{ij} + {}^2M_{rs}^{ji}\right)p_{j0}\phi_i^{\mathrm{II}}\phi_s^{\mathrm{II}}\left(A_1^{\mathrm{II}}\right)^2 \\ &- \Psi_{\mathrm{II}}^2\left({}^1D_{rs}^i + {}^2D_{rs}^{ij}p_{j0}\right)\phi_i^{\mathrm{II}}\phi_s^{\mathrm{II}}\left(A_1^{\mathrm{II}}\right)^2 \\ &- \left[{}^1K_{rs}^i + \left({}^2K_{rs}^{ij} + {}^2K_{rs}^{ji} + {}^2K_{rj}^{si}\right)p_{j0}\right]\phi_i^{\mathrm{II}}\phi_s^{\mathrm{II}}\left(A_1^{\mathrm{II}}\right)^2. \end{aligned} \tag{26}$$

Therefore

$$B_{s2}^{\mathrm{II}} = \rho_s^{\mathrm{II}}\left(A_1^{\mathrm{II}}\right)^2 = \left(\epsilon_s^{\mathrm{II}} + \mathrm{i}\xi_s^{\mathrm{II}}\right)\left(A_1^{\mathrm{II}}\right)^2 \tag{27}$$

where ϵ_s^{II} and ξ_s^{II} are real numbers.

2.2.5. Terms in $e^{(\Psi_I+\Psi_{II})T_0}$

$$\begin{aligned}
&\left[(\Psi_{\mathrm{I}}+\Psi_{\mathrm{II}})^{2}{}^{0}M^{*}_{rs}+(\Psi_{\mathrm{I}}+\Psi_{\mathrm{II}})^{0}D^{*}_{rs}+{}^{0}K^{*}_{rs}\right]C_{s2}\\
&\quad=-\Psi^{2}_{\mathrm{II}}{}^{1}M^{i}_{rs}\phi^{\mathrm{I}}_{i}\phi^{\mathrm{II}}_{s}A^{\mathrm{I}}_{1}A^{\mathrm{II}}_{1}-\Psi^{2}_{\mathrm{I}}{}^{1}M^{s}_{ri}\phi^{\mathrm{I}}_{i}\phi^{\mathrm{II}}_{s}A^{\mathrm{I}}_{1}A^{\mathrm{II}}_{1}\\
&\qquad-\left(\Psi^{2}_{\mathrm{II}}\phi^{\mathrm{I}}_{i}\phi^{\mathrm{II}}_{s}+\Psi^{2}_{\mathrm{I}}\phi^{\mathrm{I}}_{s}\phi^{\mathrm{II}}_{i}\right)\left({}^{2}M^{ij}_{rs}+{}^{2}M^{ji}_{rs}\right)p_{j0}A^{\mathrm{I}}_{1}A^{\mathrm{II}}_{1}\\
&\qquad-\Psi_{\mathrm{I}}\Psi_{\mathrm{II}}x\left({}^{1}D^{i}_{rs}+{}^{2}D^{ij}_{rs}p_{j0}\right)\left(\phi^{\mathrm{I}}_{i}\phi^{\mathrm{II}}_{s}+\phi^{\mathrm{I}}_{s}\phi^{\mathrm{II}}_{i}\right)A^{\mathrm{I}}_{1}A^{\mathrm{II}}_{1}\\
&\qquad-\left[{}^{1}K^{i}_{rs}+\left({}^{2}K^{ij}_{rs}+{}^{2}K^{ji}_{rs}+{}^{2}K^{si}_{rj}\right)p_{j0}\right]\left(\phi^{\mathrm{I}}_{i}\phi^{\mathrm{II}}_{s}+\phi^{\mathrm{I}}_{s}\phi^{\mathrm{II}}_{i}\right)A^{\mathrm{I}}_{1}A^{\mathrm{II}}_{1}.
\end{aligned}\tag{28}$$

Therefore

$$C_{s2}=\eta_{s}A^{\mathrm{I}}_{1}A^{\mathrm{II}}_{1}=(\sigma_{s}+\mathrm{i}\tau_{s})A^{\mathrm{I}}_{1}A^{\mathrm{II}}_{1}\tag{29}$$

where σ_s and τ_s are real numbers.

2.2.6. Terms in $e^{2\alpha_I T_0}$

$$\begin{aligned}
\left(4\alpha^{2}_{\mathrm{I}}{}^{0}M^{*}_{rs}+2\alpha_{\mathrm{I}}{}^{0}D^{*}_{rs}+{}^{0}K^{*}_{rs}\right)F^{\mathrm{I}}_{s2}&=-\Psi^{2}_{\mathrm{I}}\left[{}^{1}M^{i}_{rs}+\left({}^{2}M^{ij}_{rs}+{}^{2}M^{ji}_{rs}\right)p_{j0}\right]\bar{\phi}^{\mathrm{I}}_{i}\phi^{\mathrm{I}}_{s}\bar{A}^{\mathrm{I}}_{1}A^{\mathrm{I}}_{1}\\
&\quad-\Psi_{\mathrm{I}}\overline{\Psi}_{\mathrm{I}}\left({}^{1}D^{i}_{rs}+{}^{2}D^{ij}_{rs}p_{j0}\right)\bar{\phi}^{\mathrm{I}}_{i}\phi^{\mathrm{I}}_{s}\bar{A}^{\mathrm{I}}_{1}A^{\mathrm{I}}_{1}\\
&\quad-\left[{}^{1}K^{i}_{rs}+\left({}^{2}K^{ij}_{rs}+{}^{2}K^{ji}_{rs}+{}^{2}K^{si}_{rj}\right)p_{j0}\right]\bar{\phi}^{\mathrm{I}}_{i}\phi^{\mathrm{I}}_{s}\bar{A}^{\mathrm{I}}_{1}A^{\mathrm{I}}_{1}.
\end{aligned}\tag{30}$$

Therefore

$$F^{\mathrm{I}}_{s2}=\lambda^{\mathrm{I}}_{s}\bar{A}^{\mathrm{I}}_{1}A^{\mathrm{I}}_{1}=\left(\mu^{\mathrm{I}}_{s}+\mathrm{i}\upsilon^{\mathrm{I}}_{s}\right)\bar{A}^{\mathrm{I}}_{1}A^{\mathrm{I}}_{1}\tag{31}$$

where μ^{I}_{s} and $\upsilon^{\mathrm{I}}_{s}$ are real numbers.

2.2.7. Terms in $e^{2\alpha_{II} T_0}$

$$\begin{aligned}
\left(4\alpha^{2}_{\mathrm{II}}{}^{0}M^{*}_{rs}+2\alpha_{\mathrm{II}}{}^{0}D^{*}_{rs}+{}^{0}K^{*}_{rs}\right)F^{\mathrm{II}}_{s2}&=-\Psi^{2}_{\mathrm{II}}{}^{1}M^{i}_{rs}\bar{\phi}^{\mathrm{II}}_{i}\phi^{\mathrm{II}}_{s}\bar{A}^{\mathrm{II}}_{1}A^{\mathrm{II}}_{1}-\Psi^{2}_{\mathrm{II}}\left({}^{2}M^{ij}_{rs}+{}^{2}M^{ji}_{rs}\right)p_{j0}\bar{\phi}^{\mathrm{II}}_{i}\phi^{\mathrm{II}}_{s}\bar{A}^{\mathrm{II}}_{1}A^{\mathrm{II}}_{1}\\
&\quad-\Psi_{\mathrm{II}}\overline{\Psi}_{\mathrm{II}}\left({}^{1}D^{i}_{rs}+{}^{2}D^{ij}_{rs}p_{j0}\right)\bar{\phi}^{\mathrm{II}}_{i}\phi^{\mathrm{II}}_{s}\bar{A}^{\mathrm{II}}_{1}A^{\mathrm{II}}_{1}\\
&\quad-\left[{}^{1}K^{i}_{rs}+\left({}^{2}K^{ij}_{rs}+{}^{2}K^{ji}_{rs}+{}^{2}K^{si}_{rj}\right)p_{j0}\right]\bar{\phi}^{\mathrm{II}}_{i}\phi^{\mathrm{II}}_{s}\bar{A}^{\mathrm{II}}_{1}A^{\mathrm{II}}_{1}.
\end{aligned}\tag{32}$$

Therefore

$$F^{\mathrm{II}}_{s2}=\lambda^{\mathrm{II}}_{s}\bar{A}^{\mathrm{II}}_{1}A^{\mathrm{II}}_{1}=\left(\mu^{\mathrm{II}}_{s}+\mathrm{i}\nu^{\mathrm{II}}_{s}\right)\bar{A}^{\mathrm{II}}_{1}A^{\mathrm{II}}_{1}\tag{33}$$

where μ^{II}_{s} and ν^{II}_{s} are real numbers.

2.3. Overall synthesis

After integrating system (24), order ε terms in the power expansion of (3) will be determined. Also, taking into account (23), all relevant coefficients of the order ε^2 solution will be known, from (27), (29), (31) and (33). Note that terms in $e^{\Psi_1 T_0}$ and $e^{\Psi_{\mathrm{II}} T_0}$ in (18) can be neglected, since they can be included in the corresponding terms of the order ε solution. Of course, the expansion could be developed further to the order ε^3 solution and on, but the mathematics would be too costly, specially because the main qualitative features of the 1:2 internal resonance would already be captured. Of course, truncation of cubic non-linearities may have quantitative influence in the output. Anyhow, after some simplifications, the non-linear multi-mode

would be characterised by the time functions of each generalised co-ordinate p_s (and, by derivation, each generalised velocity $\dot{p}_s$)

$$\begin{aligned}
p_s = p_{s0} &+ \varepsilon\left[\frac{\left(\gamma_s^{\mathrm{I}} + \mathrm{i}\delta_s^{\mathrm{I}}\right)}{2} a_{\mathrm{I}} \mathrm{e}^{\alpha_{\mathrm{I}} t} \mathrm{e}^{\mathrm{i}(\beta_{\mathrm{I}} t + \theta_{\mathrm{I}})} + \frac{\left(\gamma_s^{\mathrm{I}} - \mathrm{i}\delta_s^{\mathrm{I}}\right)}{2} a_{\mathrm{I}} \mathrm{e}^{\alpha_{\mathrm{I}} t} \mathrm{e}^{-\mathrm{i}(\beta_{\mathrm{I}} t + \theta_{\mathrm{I}})}\right] \\
&+ \varepsilon\left[\frac{\left(\gamma_s^{\mathrm{II}} + \mathrm{i}\delta_s^{\mathrm{II}}\right)}{2} a_{\mathrm{II}} \mathrm{e}^{\alpha_{\mathrm{II}} t} \mathrm{e}^{\mathrm{i}(\beta_{\mathrm{II}} t + \theta_{\mathrm{II}})} + \frac{\left(\gamma_s^{\mathrm{II}} - \mathrm{i}\delta_s^{\mathrm{II}}\right)}{2} a_{\mathrm{II}} \mathrm{e}^{\alpha_{\mathrm{II}} t} \mathrm{e}^{-\mathrm{i}(\beta_{\mathrm{II}} t + \theta_{\mathrm{II}})}\right] + \varepsilon^2\left[\frac{\mu_s^{\mathrm{I}}}{2}(a_{\mathrm{I}})^2\right] \mathrm{e}^{2\alpha_{\mathrm{I}} t} \\
&+ \varepsilon^2\left[\frac{\mu_s^{\mathrm{II}}}{2}(a_{\mathrm{II}})^2\right] \mathrm{e}^{2\alpha_{\mathrm{II}} t} + \varepsilon^2\left[\frac{\left(\epsilon_s^{\mathrm{II}} + \mathrm{i}\xi_s^{\mathrm{II}}\right)}{4}(a_{\mathrm{II}})^2\right] \mathrm{e}^{2\alpha_{\mathrm{II}} t} \mathrm{e}^{2\mathrm{i}(\beta_{\mathrm{II}} t + \theta_{\mathrm{II}})} \\
&+ \varepsilon^2\left[\frac{\left(\epsilon_s^{\mathrm{II}} - \mathrm{i}\xi_s^{\mathrm{II}}\right)}{4}(a_{\mathrm{II}})^2\right] \mathrm{e}^{2\alpha_{\mathrm{II}} t} \mathrm{e}^{-2\mathrm{i}(\beta_{\mathrm{II}} t + \theta_{\mathrm{II}})} \varepsilon^2\left[\frac{(\sigma_s + \mathrm{i}\tau_s)}{4} a_{\mathrm{I}} a_{\mathrm{II}}\right] \mathrm{e}^{(\alpha_{\mathrm{I}} + \alpha_{\mathrm{II}}) t} \mathrm{e}^{\mathrm{i}[(\beta_{\mathrm{I}} + \beta_{\mathrm{II}}) t + (\theta_{\mathrm{I}} + \theta_{\mathrm{II}})]} \\
&+ \varepsilon^2\left[\frac{(\sigma_s - \mathrm{i}\tau_s)}{4} a_{\mathrm{I}} a_{\mathrm{II}}\right] \mathrm{e}^{(\alpha_{\mathrm{I}} + \alpha_{\mathrm{II}}) t} \mathrm{e}^{-\mathrm{i}[(\beta_{\mathrm{I}} + \beta_{\mathrm{II}}) t + (\theta_{\mathrm{I}} + \theta_{\mathrm{II}})]}
\end{aligned} \tag{34}$$

or, in real notation

$$\begin{aligned}
p_s = p_{s0} &+ \hat{a}_{\mathrm{I}} \mathrm{e}^{\alpha_{\mathrm{I}} t}\left[\gamma_s^{\mathrm{I}} \cos(\beta_{\mathrm{I}} t + \theta_{\mathrm{I}}) - \delta_s^{\mathrm{I}} \operatorname{sen}(\beta_{\mathrm{I}} t + \theta_{\mathrm{I}})\right] \\
&+ \hat{a}_{\mathrm{II}} \mathrm{e}^{\alpha_{\mathrm{II}} t}\left[\gamma_s^{\mathrm{II}} \cos(\beta_{\mathrm{II}} t + \theta_{\mathrm{II}}) - \delta_s^{\mathrm{II}} \operatorname{sen}(\beta_{\mathrm{II}} t + \theta_{\mathrm{II}})\right] + \frac{1}{2}(\hat{a}_{\mathrm{I}})^2 \mu_s^{\mathrm{I}} \mathrm{e}^{2\alpha_{\mathrm{I}} t} \\
&+ \frac{1}{2}(\hat{a}_{\mathrm{II}})^2 \mu_s^{\mathrm{II}} \mathrm{e}^{2\alpha_{\mathrm{II}} t} + \frac{1}{2}(\hat{a}_{\mathrm{II}})^2 \mathrm{e}^{2\alpha_{\mathrm{II}} t}\left[\epsilon_s^{\mathrm{II}} \cos 2(\beta_{\mathrm{II}} t + \theta_{\mathrm{II}}) - \xi_s^{\mathrm{II}} \operatorname{sen} 2(\beta_{\mathrm{II}} t + \theta_{\mathrm{II}})\right] \\
&+ \frac{1}{2}\hat{a}_{\mathrm{I}} \hat{a}_{\mathrm{II}} \mathrm{e}^{(\alpha_{\mathrm{I}} + \alpha_{\mathrm{II}}) t} \sigma_s \cos\left[(\beta_{\mathrm{I}} + \beta_{\mathrm{II}}) t + (\theta_{\mathrm{I}} + \theta_{\mathrm{II}})\right] \\
&- \frac{1}{2}\hat{a}_{\mathrm{I}} \hat{a}_{\mathrm{II}} \mathrm{e}^{(\alpha_{\mathrm{I}} + \alpha_{\mathrm{II}}) t} \tau_s \operatorname{sen}[(\beta_{\mathrm{I}} + \beta_{\mathrm{II}}) t + (\theta_{\mathrm{I}} + \theta_{\mathrm{II}})],
\end{aligned} \tag{35}$$

where $\hat{a}_{\mathrm{I}} = \varepsilon a_{\mathrm{I}}$ and $\hat{a}_{\mathrm{II}} = \varepsilon a_{\mathrm{II}}$. For details, refer to Baracho Neto (2003).

3. Non-linear multi-mode for 1:2 internal resonance: invariant manifold

To emphasise the topological structure of the non-linear multi-modes, the associated four-dimensional invariant manifold will be explicitly determined in this section from the time response obtained in the previous section. Note that a four-dimensional "surface" will be determined in the phase space, so that once the system is set to vibrate with initial conditions on this "surface", it will describe phase trajectories wholly constrained to this "surface", thus justifying the denomination "invariant" manifold. From (34) it is written

$$\begin{aligned}
p_s = p_{s0} &+ \frac{\varepsilon}{2}\left(\gamma_s^{\mathrm{I}} + \mathrm{i}\delta_s^{\mathrm{I}}\right) a_{\mathrm{I}} \mathrm{e}^{\alpha_{\mathrm{I}} t} \mathrm{e}^{\mathrm{i}\omega_{\mathrm{I}}} + \frac{\varepsilon}{2}\left(\gamma_s^{\mathrm{II}} + \mathrm{i}\delta_s^{\mathrm{II}}\right) a_{\mathrm{II}} \mathrm{e}^{\alpha_{\mathrm{II}} t} \mathrm{e}^{\mathrm{i}\omega_{\mathrm{II}}} + \frac{\varepsilon^2}{4}\left(\mu_s^{\mathrm{I}} + \mathrm{i}\nu_s^{\mathrm{I}}\right)(a_{\mathrm{I}})^2 \mathrm{e}^{2\alpha_{\mathrm{I}} t} \\
&+ \frac{\varepsilon^2}{4}\left(\mu_s^{\mathrm{II}} + \mathrm{i}\nu_s^{\mathrm{II}}\right)(a_{\mathrm{II}})^2 \mathrm{e}^{2\alpha_{\mathrm{II}} t} + \frac{\varepsilon^2}{4}\left(\epsilon_s^{\mathrm{II}} + \mathrm{i}\xi_s^{\mathrm{II}}\right)(a_{\mathrm{II}})^2 \mathrm{e}^{2\alpha_{\mathrm{II}} t} \mathrm{e}^{\mathrm{i}2\omega_{\mathrm{II}}} \\
&+ \frac{\varepsilon^2}{4}(\sigma_s + \mathrm{i}\tau_s) a_{\mathrm{I}} a_{\mathrm{II}} \mathrm{e}^{(\alpha_{\mathrm{I}} + \alpha_{\mathrm{II}}) t} \mathrm{e}^{\mathrm{i}(\omega_{\mathrm{I}} + \omega_{\mathrm{II}})} + \text{c.c.}
\end{aligned} \tag{36}$$

with

$$\begin{aligned}\omega_{\mathrm{I}} &= \beta_{\mathrm{I}} t + \theta_{\mathrm{I}} \\ \omega_{\mathrm{II}} &= \beta_{\mathrm{II}} t + \theta_{\mathrm{II}}\end{aligned} \tag{37}$$

The generalised velocities can be obtained by derivation with respect to time, according to

$$\frac{\mathrm{d}p_s}{\mathrm{d}t} = \dot{p}_s = D_0 p_s + \varepsilon D_1 p_s + \mathcal{O}(\varepsilon^3) \tag{38}$$

Hence

$$\begin{aligned}\dot{p}_s = {} & \frac{\varepsilon}{2}\left(\gamma_s^{\mathrm{I}} + \mathrm{i}\delta_s^{\mathrm{I}}\right)(\alpha_{\mathrm{I}} + \mathrm{i}\beta_{\mathrm{I}}) a_{\mathrm{I}} \mathrm{e}^{\alpha_{\mathrm{I}} t}\mathrm{e}^{\mathrm{i}\omega_{\mathrm{I}}} + \frac{\varepsilon}{2}\left(\gamma_s^{\mathrm{II}} + \mathrm{i}\delta_s^{\mathrm{II}}\right)(\alpha_{\mathrm{II}} + \mathrm{i}\beta_{\mathrm{II}}) a_{\mathrm{II}} \mathrm{e}^{\alpha_{\mathrm{II}} t}\mathrm{e}^{\mathrm{i}\omega_{\mathrm{II}}} + \frac{\varepsilon^2}{2}\left(\mu_s^{\mathrm{I}} + \mathrm{i}\nu_s^{\mathrm{I}}\right)\alpha_{\mathrm{I}}(a_{\mathrm{I}})^2 \mathrm{e}^{2\alpha_{\mathrm{I}} t} \\ & + \frac{\varepsilon^2}{2}\left(\mu_s^{\mathrm{II}} + \mathrm{i}\nu_s^{\mathrm{II}}\right)\alpha_{\mathrm{II}}(a_{\mathrm{II}})^2 \mathrm{e}^{2\alpha_{\mathrm{II}} t} + \frac{\varepsilon^2}{2}\left(\epsilon_s^{\mathrm{II}} + \mathrm{i}\xi_s^{\mathrm{II}}\right)(\alpha_{\mathrm{II}} + \mathrm{i}\beta_{\mathrm{II}})(a_{\mathrm{II}})^2 \mathrm{e}^{2\alpha_{\mathrm{II}} t}\mathrm{e}^{\mathrm{i}2\omega_{\mathrm{II}}} \\ & + \frac{\varepsilon^2}{4}(\sigma_s + \mathrm{i}\tau_s)[(\alpha_{\mathrm{I}} + \alpha_{\mathrm{II}}) + i(\beta_{\mathrm{I}} + \beta_{\mathrm{II}})] a_{\mathrm{I}} a_{\mathrm{II}} \mathrm{e}^{(\alpha_{\mathrm{I}} + \alpha_{\mathrm{II}})t}\mathrm{e}^{\mathrm{i}(\omega_{\mathrm{I}} + \omega_{\mathrm{II}})} - \frac{\varepsilon^2}{4}\left(\gamma_s^{\mathrm{I}} + \mathrm{i}\delta_s^{\mathrm{I}}\right)\bar{a} a_{\mathrm{I}} a_{\mathrm{II}} \mathrm{e}^{(\alpha_{\mathrm{I}} + \alpha_{\mathrm{II}})t}\mathrm{e}^{\mathrm{i}\omega_{\mathrm{I}}} \\ & - \frac{\varepsilon^2}{4}\left(\gamma_s^{\mathrm{II}} + \mathrm{i}\delta_s^{\mathrm{II}}\right)\bar{b}(a_{\mathrm{I}})^2 \mathrm{e}^{2\alpha_{\mathrm{I}} t}\mathrm{e}^{\mathrm{i}\omega_{\mathrm{II}}} + \text{c.c.}\end{aligned} \tag{39}$$

where

$$\bar{a} = \frac{1}{\left[(a_1)^2 + (b_1)^2\right]}\left[(a_1 c_1 + b_1 d_1)\cos\gamma_1 + (b_1 c_1 - a_1 d_1)\,\mathrm{sen}\,\gamma_1\right] \tag{40}$$

$$\bar{b} = \frac{1}{\left[(a_2)^2 + (b_2)^2\right]}\left[(a_2 c_2 + b_2 d_2)\cos\gamma_1 - (b_2 c_2 - a_2 d_2)\,\mathrm{sen}\,\gamma_1\right]. \tag{41}$$

It is meant to describe the four-dimensional invariant manifold in terms of the modal variables U_1, V_1, U_2 and V_2, as indicated by

$$\begin{aligned}p_s = {} & p_{s0} + F_{s1}U_1 + F_{s2}U_2 + F_{s3}V_1 + F_{s4}V_2 + F_{s5}(U_1)^2 + F_{s6}(U_2)^2 + F_{s7}U_1U_2 + F_{s8}U_1V_1 \\ & + F_{s9}U_2V_2 + F_{s10}U_1V_2 + F_{s11}U_2V_1 + F_{s12}(V_1)^2 + F_{s13}(V_2)^2 + F_{s14}V_1V_2 \\ \dot{p}_s = {} & G_{s1}U_1 + G_{s2}U_2 + G_{s3}V_1 + G_{s4}V_2 + G_{s5}(U_1)^2 + G_{s6}(U_2)^2 + G_{s7}U_1U_2 + G_{s8}U_1V_1 \\ & + G_{s9}U_2V_2 + G_{s10}U_1V_2 + G_{s11}U_2V_1 + G_{s12}(V_1)^2 + G_{s13}(V_2)^2 + G_{s14}V_1V_2.\end{aligned} \tag{42}$$

Any two pairs of generalised co-ordinates (such as p_v and p_w) and velocities (such as $\dot{p}_v$ and $\dot{p}_w$) can be used to define the modal amplitudes (U_1, U_2, V_1 and V_2, respectively), provided they are not identically null. The modal amplitudes time responses are explicitly given by the following expressions, once the initial conditions are set

$$\begin{aligned}U_1 = {} & p_v - p_{v0} \\ = {} & \frac{\varepsilon}{2} a_{\mathrm{I}} \mathrm{e}^{\alpha_{\mathrm{I}} t}\mathrm{e}^{\mathrm{i}\omega_{\mathrm{I}}} + \frac{\varepsilon}{2}\left(\gamma_v^{\mathrm{II}} + \mathrm{i}\delta_v^{\mathrm{II}}\right) a_{\mathrm{II}} \mathrm{e}^{\alpha_{\mathrm{II}} t}\mathrm{e}^{\mathrm{i}\omega_{\mathrm{II}}} + \frac{\varepsilon^2}{4}\left(\mu_v^{\mathrm{I}} + \mathrm{i}\nu_v^{\mathrm{I}}\right)(a_{\mathrm{I}})^2 \mathrm{e}^{2\alpha_{\mathrm{I}} t} + \frac{\varepsilon^2}{4}\left(\mu_v^{\mathrm{II}} + \mathrm{i}\nu_v^{\mathrm{II}}\right)(a_{\mathrm{II}})^2 \mathrm{e}^{2\alpha_{\mathrm{II}} t} \\ & + \frac{\varepsilon^2}{4}\left(\epsilon_v^{\mathrm{II}} + \mathrm{i}\xi_v^{\mathrm{II}}\right)(a_{\mathrm{II}})^2 \mathrm{e}^{2\alpha_{\mathrm{II}} t}\mathrm{e}^{\mathrm{i}2\omega_{\mathrm{II}}} + \frac{\varepsilon^2}{4}(\sigma_v + \mathrm{i}\tau_v) a_{\mathrm{I}} a_{\mathrm{II}} \mathrm{e}^{(\alpha_{\mathrm{I}} + \alpha_{\mathrm{II}})t}\mathrm{e}^{\mathrm{i}(\omega_{\mathrm{I}} + \omega_{\mathrm{II}})} + \text{c.c.}\end{aligned}$$

$$
\begin{aligned}
V_1 &= \dot{p}_v \\
&= \frac{\varepsilon}{2}(\alpha_{\mathrm{I}} + \mathrm{i}\beta_{\mathrm{I}})a_{\mathrm{I}}\mathrm{e}^{\alpha_{\mathrm{I}}t}\mathrm{e}^{\mathrm{i}\omega_{\mathrm{I}}} + \frac{\varepsilon}{2}\left(\gamma_v^{\mathrm{II}} + \mathrm{i}\delta_v^{\mathrm{II}}\right)(\alpha_{\mathrm{II}} + \mathrm{i}\beta_{\mathrm{II}})a_{\mathrm{II}}\mathrm{e}^{\alpha_{\mathrm{II}}t}\mathrm{e}^{\mathrm{i}\omega_{\mathrm{II}}} + \frac{\varepsilon^2}{2}\left(\mu_v^{\mathrm{I}} + \mathrm{i}\nu_v^{\mathrm{I}}\right)\alpha_{\mathrm{I}}(a_{\mathrm{I}})^2\mathrm{e}^{2\alpha_{\mathrm{I}}t} \\
&\quad + \frac{\varepsilon^2}{2}\left(\mu_v^{\mathrm{II}} + \mathrm{i}\nu_v^{\mathrm{II}}\right)\alpha_{\mathrm{II}}(a_{\mathrm{II}})^2\mathrm{e}^{2\alpha_{\mathrm{II}}t} + \frac{\varepsilon^2}{2}\left(\epsilon_v^{\mathrm{II}} + \mathrm{i}\xi_v^{\mathrm{II}}\right)(\alpha_{\mathrm{II}} + \mathrm{i}\beta_{\mathrm{II}})(a_{\mathrm{II}})^2\mathrm{e}^{2\alpha_{\mathrm{II}}t}\mathrm{e}^{\mathrm{i}2\omega_{\mathrm{II}}} \\
&\quad + \frac{\varepsilon^2}{4}(\sigma_v + \mathrm{i}\tau_v)[(\alpha_{\mathrm{I}} + \alpha_{\mathrm{II}}) + i(\beta_{\mathrm{I}} + \beta_{\mathrm{II}})]a_{\mathrm{I}}a_{\mathrm{II}}\mathrm{e}^{(\alpha_{\mathrm{I}}+\alpha_{\mathrm{II}})t}\mathrm{e}^{\mathrm{i}(\omega_{\mathrm{I}}+\omega_{\mathrm{II}})} \\
&\quad - \frac{\varepsilon^2}{4}\left(\gamma_v^{\mathrm{I}} + \mathrm{i}\delta_v^{\mathrm{I}}\right)\bar{a}a_{\mathrm{I}}a_{\mathrm{II}}\mathrm{e}^{(\alpha_{\mathrm{I}}+\alpha_{\mathrm{II}})t}\mathrm{e}^{\mathrm{i}\omega_{\mathrm{I}}} - \frac{\varepsilon^2}{4}\left(\gamma_v^{\mathrm{II}} + \mathrm{i}\delta_v^{\mathrm{II}}\right)\bar{b}(a_{\mathrm{I}})^2\mathrm{e}^{2\alpha_{\mathrm{I}}t}\mathrm{e}^{\mathrm{i}\omega_{\mathrm{II}}} + \text{c.c.}
\end{aligned} \tag{43}
$$

$$
\begin{aligned}
U_2 &= p_w - p_{w0} = \frac{\varepsilon}{2}\left(\gamma_w^{\mathrm{I}} + \mathrm{i}\delta_w^{\mathrm{I}}\right)a_{\mathrm{I}}\mathrm{e}^{\alpha_{\mathrm{I}}t}\mathrm{e}^{\mathrm{i}\omega_{\mathrm{I}}} + \frac{\varepsilon}{2}a_{\mathrm{II}}\mathrm{e}^{\alpha_{\mathrm{II}}t}\mathrm{e}^{\mathrm{i}\omega_{\mathrm{II}}} + \frac{\varepsilon^2}{4}\left(\mu_w^{\mathrm{I}} + \mathrm{i}\nu_w^{\mathrm{I}}\right)(a_{\mathrm{I}})^2\mathrm{e}^{2\alpha_{\mathrm{I}}t} + \frac{\varepsilon^2}{4}\left(\mu_w^{\mathrm{II}} + \mathrm{i}\nu_w^{\mathrm{II}}\right)(a_{\mathrm{II}})^2\mathrm{e}^{2\alpha_{\mathrm{II}}t} \\
&\quad + \frac{\varepsilon^2}{4}\left(\epsilon_w^{\mathrm{II}} + \mathrm{i}\xi_w^{\mathrm{II}}\right)(a_{\mathrm{II}})^2\mathrm{e}^{2\alpha_{\mathrm{II}}t}\mathrm{e}^{\mathrm{i}2\omega_{\mathrm{II}}} + \frac{\varepsilon^2}{4}(\sigma_w + \mathrm{i}\tau_w)a_{\mathrm{I}}a_{\mathrm{II}}\mathrm{e}^{(\alpha_{\mathrm{I}}+\alpha_{\mathrm{II}})t}\mathrm{e}^{\mathrm{i}(\omega_{\mathrm{I}}+\omega_{\mathrm{II}})} + \text{c.c.}
\end{aligned}
$$

$$
\begin{aligned}
V_2 &= \dot{p}_w = \frac{\varepsilon}{2}\left(\gamma_w^{\mathrm{I}} + \mathrm{i}\delta_w^{\mathrm{I}}\right)(\alpha_{\mathrm{I}} + \mathrm{i}\beta_{\mathrm{I}})a_{\mathrm{I}}\mathrm{e}^{\alpha_{\mathrm{I}}t}\mathrm{e}^{\mathrm{i}\omega_{\mathrm{I}}} + \frac{\varepsilon}{2}(\alpha_{\mathrm{II}} + \mathrm{i}\beta_{\mathrm{II}})a_{\mathrm{II}}\mathrm{e}^{\alpha_{\mathrm{II}}t}\mathrm{e}^{\mathrm{i}\omega_{\mathrm{II}}} + \frac{\varepsilon^2}{2}\left(\mu_w^{\mathrm{I}} + \mathrm{i}\nu_w^{\mathrm{I}}\right)\alpha_{\mathrm{I}}(a_{\mathrm{I}})^2\mathrm{e}^{2\alpha_{\mathrm{I}}t} \\
&\quad + \frac{\varepsilon^2}{2}\left(\mu_w^{\mathrm{II}} + \mathrm{i}\nu_w^{\mathrm{II}}\right)\alpha_{\mathrm{II}}(a_{\mathrm{II}})^2\mathrm{e}^{2\alpha_{\mathrm{II}}t} + \frac{\varepsilon^2}{2}\left(\epsilon_w^{\mathrm{II}} + \mathrm{i}\xi_w^{\mathrm{II}}\right)(\alpha_{\mathrm{II}} + \mathrm{i}\beta_{\mathrm{II}})(a_{\mathrm{II}})^2\mathrm{e}^{2\alpha_{\mathrm{II}}t}\mathrm{e}^{\mathrm{i}2\omega_{\mathrm{II}}} \\
&\quad + \frac{\varepsilon^2}{4}(\sigma_w + \mathrm{i}\tau_w)[(\alpha_{\mathrm{I}} + \alpha_{\mathrm{II}}) + i(\beta_{\mathrm{I}} + \beta_{\mathrm{II}})]a_{\mathrm{I}}a_{\mathrm{II}}\mathrm{e}^{(\alpha_{\mathrm{I}}+\alpha_{\mathrm{II}})t}\mathrm{e}^{\mathrm{i}(\omega_{\mathrm{I}}+\omega_{\mathrm{II}})} - \frac{\varepsilon^2}{4}\left(\gamma_w^{\mathrm{I}} + \mathrm{i}\delta_w^{\mathrm{I}}\right)\bar{a}a_{\mathrm{I}}a_{\mathrm{II}}\mathrm{e}^{(\alpha_{\mathrm{I}}+\alpha_{\mathrm{II}})t}\mathrm{e}^{\mathrm{i}\omega_{\mathrm{I}}} \\
&\quad - \frac{\varepsilon^2}{4}\left(\gamma_w^{\mathrm{II}} + \mathrm{i}\delta_w^{\mathrm{II}}\right)\bar{b}(a_{\mathrm{I}})^2\mathrm{e}^{2\alpha_{\mathrm{I}}t}\mathrm{e}^{\mathrm{i}\omega_{\mathrm{II}}} + \text{c.c.}
\end{aligned} \tag{44}
$$

It remains to evaluate the coefficients F_{s1} to F_{s14} and G_{s1} to G_{s14} to each one of the degrees of freedom $s = 1,\ldots,n$. It can be accomplished following the steps: firstly, (36) and (39) are inserted into the left-hand side of (42), while (43) and (44) are inserted into the right-hand side of (42); secondly, for each order of ε, the terms on the left-hand side are identified to those on the right-hand side for each linearly independent exponential function, so that linear systems of complex equations will be obtained; thirdly, after separation of real and imaginary parts, these systems can be transformed into linear systems of real algebraic equations in the coefficients F_{s1} to F_{s14} and G_{s1} to G_{s14}, which can be finally solved. For brevity, the explict expressions for the coefficients F_{s1} to F_{s14} and G_{s1} to G_{s14} will not be shown here. The authors implemented a computational procedure to determine them, using a symbolic mathematics package. For details, refer to Baracho Neto (2003).

4. Example 1: three-degree-of-freedom quadratic oscillator

For the sake of initial benchmarking of the procedure, even before the finite-element implementation had been pursued, a few test problems were considered. This section refers to one of the very first of those tests, namely that of a three-degree-of-freedom oscillator with a quadratic-law spring, as seen in Fig. 1.

The assumed non-linear spring laws state that the spring forces are $k_i\Delta_i - \mathbb{k}_i\Delta_i^2$, $i = 1,2,3$, where Δ_i stands for the spring deformation. Hence, for positive $\mathbb{k}_i$ the spring has a softening non-linear behaviour, whereas for negative $\mathbb{k}_i$ the spring has a hardening non-linear behaviour. As for the linear viscous dampers, the dissipative forces are $c_i\dot{\Delta}_i$, $i = 1,2,3$, where $\dot{\Delta}_i$ stands for the spring deformation velocity. The following parametrisation is introduced for convenience:

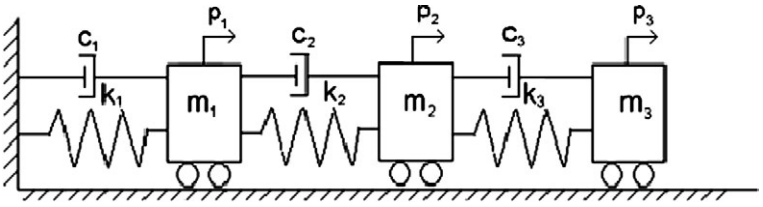

Fig. 1. Three-degree-of-freedom quadratic oscillator.

$$\begin{aligned} &m_1 = \bar{m}_1\hat{m} \quad m_2 = \bar{m}_2\hat{m} \quad m_3 = \bar{m}_3\hat{m} \\ &c_1 = \bar{c}_1 c \quad c_2 = \bar{c}_2 c \quad c_3 = \bar{c}_3 c \\ &k_1 = \bar{k}_1 k \quad k_2 = \bar{k}_2 k \quad k_3 = \bar{k}_3 k \end{aligned} \tag{45}$$

It will be seen that an adequate choice of the system parameters can be made to assure that a 1:2 internal resonance happens between the second and the third linear modes. In such conditions, the results obtained with the proposed procedure are compared with those coming out of direct numerical integration and very good agreement is observed, in terms of the time responses for each of the three degrees of freedom. It is also seen that, once two of the generalised co-ordinates are chosen as modal variables, the third co-ordinate can be expressed in terms of them, as one would expect to see, had the invariant manifold technique been used (which, by the way, is not trivial at all to apply here). It is seen that the procedure is capable of extracting such explicit analytical relationship of the third generalised co-ordinate in terms of the chosen modal variables. Moreover, the response of this extracted third generalised co-ordinate, is still in excellent agreement with the multiple scales results, as desired.

4.1. Equations of motion

The equations of motion for the three-degree-of-freedom system of Fig. 1 can be written as in (1) and (2), with

$$\begin{aligned} &\left[{}^0M\right] = \hat{m}\begin{bmatrix} \bar{m}_1 & 0 & 0 \\ 0 & \bar{m}_2 & 0 \\ 0 & 0 & \bar{m}_3 \end{bmatrix}; \quad \left[{}^0D\right] = c\begin{bmatrix} \bar{c}_1+\bar{c}_2 & -\bar{c}_2 & 0 \\ -\bar{c}_2 & \bar{c}_2+\bar{c}_3 & -\bar{c}_3 \\ 0 & -\bar{c}_3 & \bar{c}_3 \end{bmatrix}; \\ &\left[{}^0K\right] = k\begin{bmatrix} \bar{k}_1+\bar{k}_2 & -\bar{k}_2 & 0 \\ -\bar{k}_2 & \bar{k}_2+\bar{k}_3 & -\bar{k}_3 \\ 0 & -\bar{k}_3 & \bar{k}_3 \end{bmatrix} \end{aligned} \tag{46}$$

$$\begin{aligned} &\left[{}^1K^1\right] = \begin{bmatrix} -(\mathbb{k}_1-\mathbb{k}_2) & -\mathbb{k}_2 & 0 \\ -\mathbb{k}_2 & \mathbb{k}_2 & 0 \\ 0 & 0 & 0 \end{bmatrix}; \quad \left[{}^1K^2\right] = \begin{bmatrix} -\mathbb{k}_2 & \mathbb{k}_2 & 0 \\ \mathbb{k}_2 & -(\mathbb{k}_2-\mathbb{k}_3) & -\mathbb{k}_3 \\ 0 & -\mathbb{k}_3 & \mathbb{k}_3 \end{bmatrix}; \\ &\left[{}^1K^3\right] = \begin{bmatrix} 0 & 0 & 0 \\ 0 & -\mathbb{k}_3 & \mathbb{k}_3 \\ 0 & \mathbb{k}_3 & -\mathbb{k}_3 \end{bmatrix} \end{aligned} \tag{47}$$

It can be seen that the third undamped linear frequency is approximately twice the second one when the following choice of parameters is made

$$\begin{aligned} &\bar{m}_1 = 2 \quad \bar{m}_2 = \bar{m}_3 = 1 \\ &\bar{k}_1 = 1,54 \quad \bar{k}_2 = 3 \quad \bar{k}_3 = 1 \end{aligned} \tag{48}$$

In fact, the three undamped linear frequencies, in this case, are

$$\beta_1 = 0.5449 \text{ rd/s}; \quad \beta_2 = 1.1809 \text{ rd/s}; \quad \beta_3 = 2.3619 \text{ rd/s} \cong 2\beta_2 \tag{49}$$

The following parameters have also been assumed

$$\hat{m} = 1 \text{ kg}; \quad k = 1 \text{ N/m}; \quad \mathbb{k}_1 = \mathbb{k}_2 = \mathbb{k}_3 = 0.25 \text{ N/m}^2 \tag{50}$$

Two simulations are considered, a damped system and next an undamped system, just for the sake of displaying, for a longer period of time, the non-linear effects present in the multi-mode. In both simulations the generalised co-ordinates p_1 and p_2, and their time derivatives, were taken as modal variables of modes II (third mode) and I (second mode), respectively.

4.2. Damped system

For the damped system with $c = 0.1$ Ns/m and $\bar{c}_1 = \bar{c}_2 = \bar{c}_3 = 1$, evaluation of the non-linear multi-mode, coming out of the strong coupling between the second and the third linear modes, was performed following the proposed procedure. The damped frequencies ($\beta_1 = 0.5449$ rd/s, $\beta_2 = 1.1798$ rd/s and $\beta_3 = 2.3573$ rd/s $\cong 2\beta_2$) are slightly different from the undamped ones—see (49). The associated damped free-vibration responses for all generalised co-ordinates were determined, such as that shown in Fig. 2 for the generalised co-ordinate p_2, for a specified set of initial conditions $\hat{a}_{\mathrm{I}}(0) = 0.10$ m, $\hat{a}_{\mathrm{II}}(0) = 0.01$ m, $\theta_{\mathrm{I}}(0) = 0$ and $\theta_{\mathrm{II}}(0) = 0$, which lead to $p_1(0) = 0.1829$ m, $\dot{p}_1(0) = -0.0251$ m/s, $p_2(0) = 0.0799$ m, $\dot{p}_2(0) = -0.0017$ m/s, $p_3(0) = -0.2299$ m and $\dot{p}_3(0) = 0.0278$ m/s. Even in the early stages of the motion, it is already noticeable how different the linear and the non-linear solutions are. Furthermore, a good agreement is visible between the results of the proposed procedure and those of numerical integration.

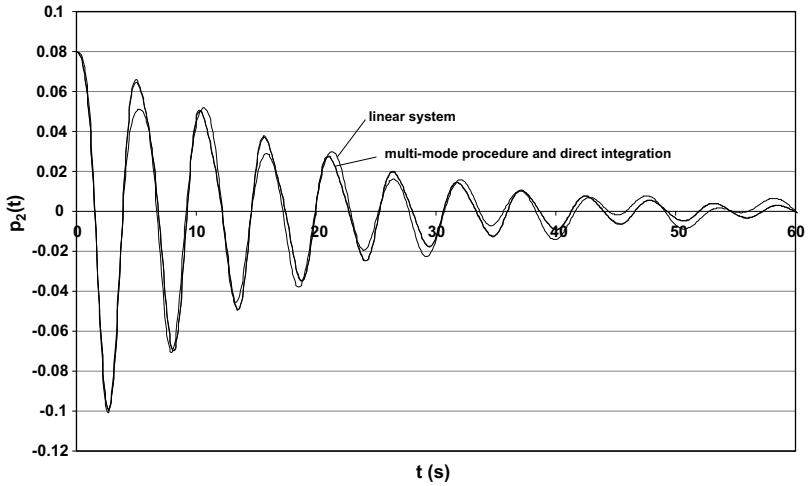

Fig. 2. Time-response $p_2(t)$ of a damped system.

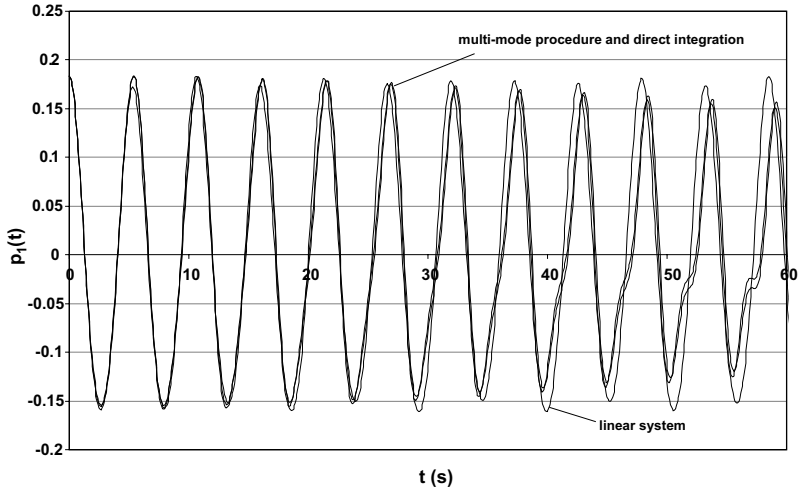

Fig. 3. Time-response $p_1(t)$ of an undamped system.

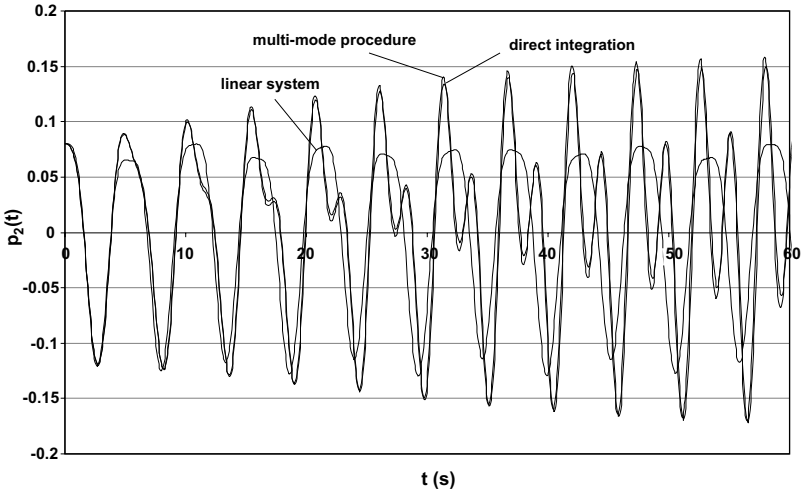

Fig. 4. Time-response $p_2(t)$ of an undamped system.

4.3. Undamped system

For the undamped system, the exchange of energy between the third and the second linear modes goes on indefinitely. Figs. 3–5 show the comparison of results among the linear analysis, multi-mode procedure and direct numerical integration. Again, even in the early stages of the motion, it is readily noticeable how different the linear and the non-linear solutions are. With regard to the multi-mode procedure, it is worthwhile mentioning that the extracted generalised co-ordinate, defined in terms of the other two generalised co-ordinates and velocities chosen as modal variables, in the manner equivalent to the invariant manifold

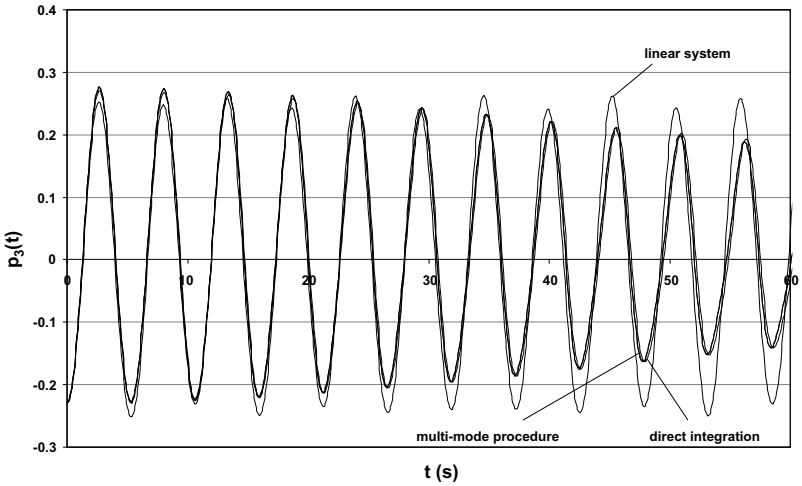

Fig. 5. Time-response $p_3(t)$ of an undamped system.

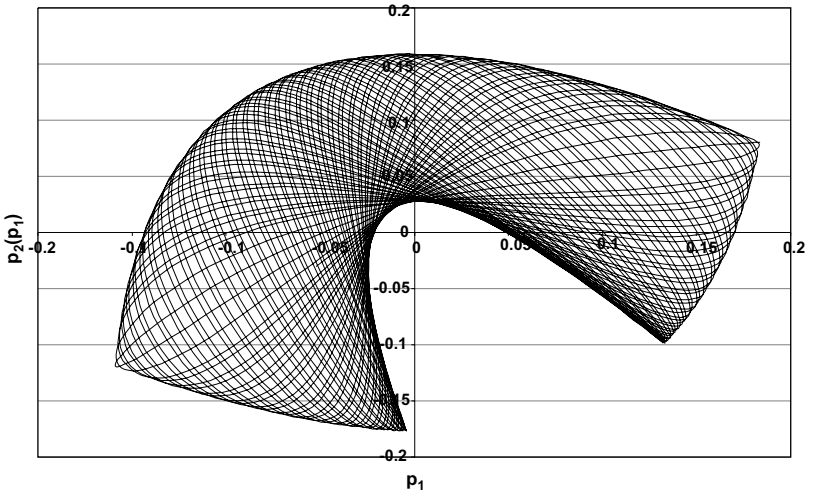

Fig. 6. Phase-trajectory projection onto the $p_1 \times p_2$ phase plane.

description of the multi-mode, agrees very well with the original time response. The initial conditions in terms of modal amplitudes and phase angles remain the same as before, that is, $\hat{a}_{\mathrm{I}}(0) = 0.10$ m, $\hat{a}_{\mathrm{II}}(0) = 0.01$ m, $\theta_{\mathrm{I}}(0) = 0$ and $\theta_{\mathrm{II}}(0) = 0$, nevertheless they are slightly different in terms of generalised co-ordinates and velocities, that is, $p_1(0) = 0.1838$ m, $\dot{p}_1(0) = 0$ m/s, $p_2(0) = 0.0802$ m, $\dot{p}_2(0) = 0$ m/s, $p_3(0) = -0.2301$ m and $\dot{p}_3(0) = 0$ m/s.

Fig. 6 displays the phase-trajectory projection from the four-dimensional invariant manifold onto the $p_1 \times p_2$ phase plane, from which it is clearly seen the non-linear aspect of the multi-mode.

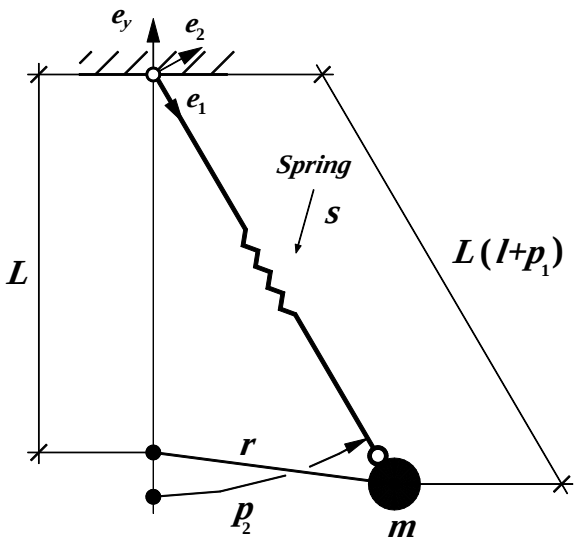

Fig. 7. Extensible pendulum.

5. Example 2: elastic pendulum

This section refers to another benchmark test, namely that of a two-degree-of-freedom undamped elastic pendulum, as seen in Fig. 7.

In this case a 1:2 internal resonance is assumed to happen between the angular and the radial modes. The results obtained with the proposed procedure are compared with those coming out of direct numerical integration and very good agreement is observed, in terms of the time responses for each of the two degrees of freedom. Analytical studies, such as those of Mazzilli (1982), showed that there is a strong interaction between the radial and the angular modes for the great majority of initial conditions. The energy imparted to one of the modes is continuously transferred to the other one along the time response. Roughly speaking, when the maximum amplitude is attained for one mode, the other one has almost null amplitude. Yet, there are particular starting conditions for which both modes have nearly simple harmonic motions in steady states, without noticeable energy exchange. Numerical simulations were performed in both cases, with good results. When the energy exchange is remarkable, it is seen that the response anticipated by the procedure for multi-mode evaluation proposed here is extremely sensitive to small numerical deviations of the generalised co-ordinates and velocities, producing a large variation upon the modulation period. As a consequence, there appears a shift between the numerical integration results and the multi-mode procedure after a few cycles.

5.1. Equations of motion

The equations of motion for the two-degree-of-freedom undamped elastic pendulum of Fig. 7, see Mazzilli (1982), can be shown to be

$$\begin{aligned} \ddot{p}_1 + \beta_1^2 p_1 + \beta_2^2(1-\cos p_2) - (1+p_1)\dot{p}_2^2 &= 0 \\ (1+p_1)^2\ddot{p}_2 + 2(1+p_1)\dot{p}_1\dot{p}_2 + \beta_2^2(1+p_1)\operatorname{sen} p_2 &= 0 \end{aligned} \tag{51}$$

where parameters s (spring stiffness), m (suspended mass) and L (pendulum length) are chosen so that

$$\beta_1 = \sqrt{\frac{s}{m}} = 9.050 \text{ rd/s} = 2\beta_2; \quad \beta_2 = \sqrt{\frac{g}{L}} = 4.525 \text{ rd/s} \tag{52}$$

If non-linearities up to the quadratic order are kept, a simpler non-linear set of differential equations can be used instead of (51)

$$\begin{aligned} &\ddot{p}_1 + \beta_1^2 p_1 + \frac{1}{2}\beta_2^2 p_2^2 - \dot{p}_2^2 = 0 \\ &\ddot{p}_2 + \beta_2^2 p_2 + \beta_2^2 p_1 p_2 + 2p_1\ddot{p}_2 + 2\dot{p}_1\dot{p}_2 = 0 \end{aligned} \tag{53}$$

According to the notation used in (1) and (2), the following matrices can be recognised, all the other ones being null

$$\left[{}^0M\right] = \begin{bmatrix} 1 & 0 \\ 0 & 1 \end{bmatrix}; \quad \left[{}^0K\right] = \begin{bmatrix} \beta_1^2 & 0 \\ 0 & \beta_2^2 \end{bmatrix} \tag{54}$$

$$\begin{aligned} \left[{}^1M^1\right] &= \begin{bmatrix} 0 & 0 \\ 0 & 2 \end{bmatrix} \\ \left[{}^1D^1\right] &= \begin{bmatrix} 0 & 0 \\ 0 & 1 \end{bmatrix}; \quad \left[{}^1D^2\right] = \begin{bmatrix} 0 & -1 \\ 1 & 0 \end{bmatrix} \\ \left[{}^1K^1\right] &= \begin{bmatrix} 0 & 0 \\ 0 & \frac{\beta_2^2}{2} \end{bmatrix}; \quad \left[{}^1K^2\right] = \begin{bmatrix} 0 & \frac{\beta_2^2}{2} \\ \frac{\beta_2^2}{2} & 0 \end{bmatrix} \end{aligned} \tag{55}$$

The generalised co-ordinate p_2 and its corresponding velocity $\dot{p}_2$ were taken as modal variables of the lower frequency mode ($\beta_{\mathrm{I}} = \beta_2 = 4.525$ rd/s), whereas p_1 and its corresponding velocity $\dot{p}_1$ were taken as modal variables of the higher frequency mode ($\beta_{\mathrm{II}} = \beta_1 = 9.050$ rd/s). Two simulations are discussed in what follows, for rather different physical situations concerning the energy exchange between the resonating modes.

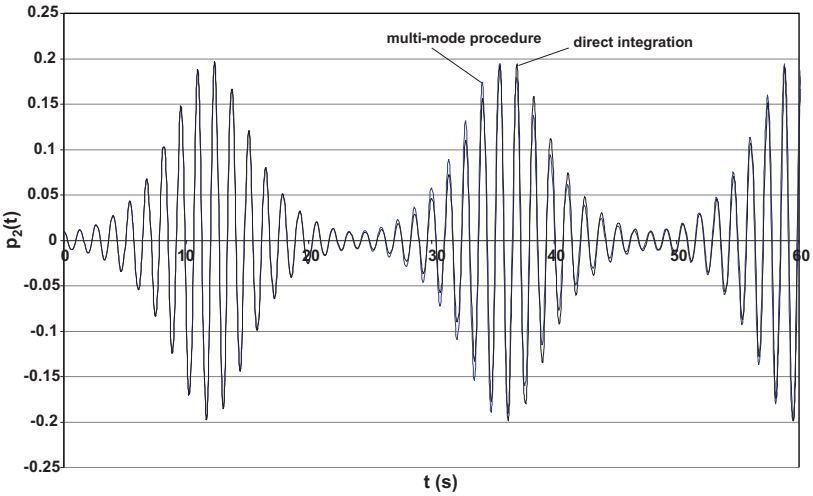

Fig. 8. Time-response for $p_2(t)$ co-ordinate.

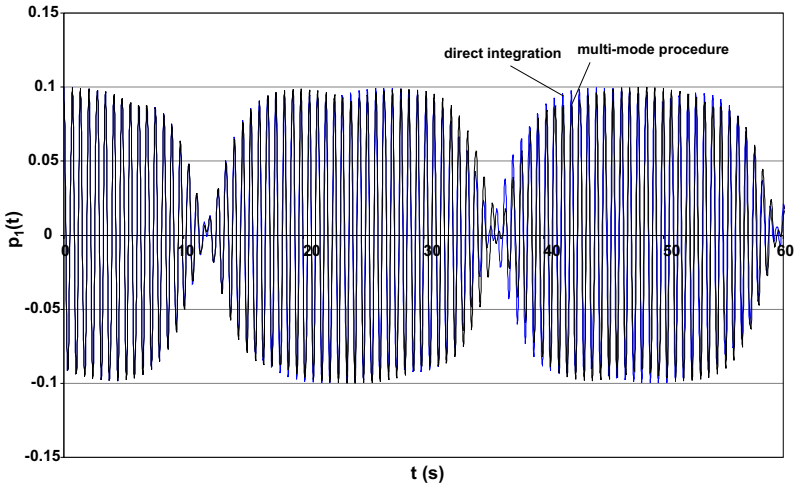

Fig. 9. Time-response for $p_1(t)$ co-ordinate.

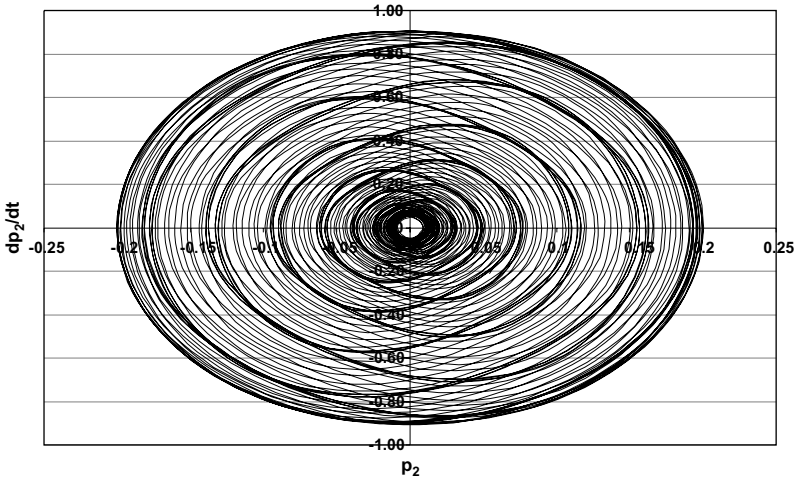

Fig. 10. Phase-trajectory projection onto the $\dot{p}_2 \times p_2$ phase plane.

5.2. First simulation: large energy exchange

The first numerical simulation corresponds to the case of strong energy exchange between the two resonating modes, resulting in a "beating" or modulation effect in the time responses, as seen in Figs. 8 and 9. In order to perform this study, the initial conditions were set to $\hat{a}_{\mathrm{I}}(0) = 0.01$, $\hat{a}_{\mathrm{II}}(0) = 0.10$, $\theta_{\mathrm{I}}(0) = 0$ and $\theta_{\mathrm{II}}(0) = 0$, which lead to $p_1(0) = 0.1000$, $\dot{p}_1(0) = 0$, $p_2(0) = 0.0097$ and $\dot{p}_2(0) = 0$.

Note that in this model there are also cubic non-linearities, besides the quadratic ones. Due to the truncation of the time response expansions for orders larger than ε^2, small quantitative discrepancies should be expected. In fact, numerical integration does show slight shifts in the time responses, as compared to the multiple-scale results, for large times (here, for $t \geqslant 100$ s), although the amplitudes still agree well. This suggests that small differences arise between the numerical and analytical estimates for θ_{I} and θ_{II}, which correct

the frequency estimates. It is also seen a small difference in the period of amplitude modulation, or "beating period". Even so, projections of phase trajectories—embedded on the four-dimensional invariant manifold—onto a phase plane, such as $\dot{p}_2 \times p_2$ in Fig. 10, agree very well for both the numerical and the analytical solution.

5.3. Second simulation: negligible energy exchange

The second numerical simulation illustrates the case of a quasi-harmonic steady state, as result of a particular choice of initial conditions—see Mazzilli (1982)—, as seen in Figs. 11 and 12. In order to perform this study, the initial conditions were set to $\hat{a}_{\mathrm{I}}(0) = 0.2829$, $\hat{a}_{\mathrm{II}}(0) = 0.1000$, $\theta_{\mathrm{I}}(0) = 0$ and $\theta_{\mathrm{II}}(0) = 0$, which lead to $p_1(0) = 0.1050$, $\dot{p}_1(0) = 0$, $p_2(0) = 0.2740$ and $\dot{p}_2(0) = 0$.

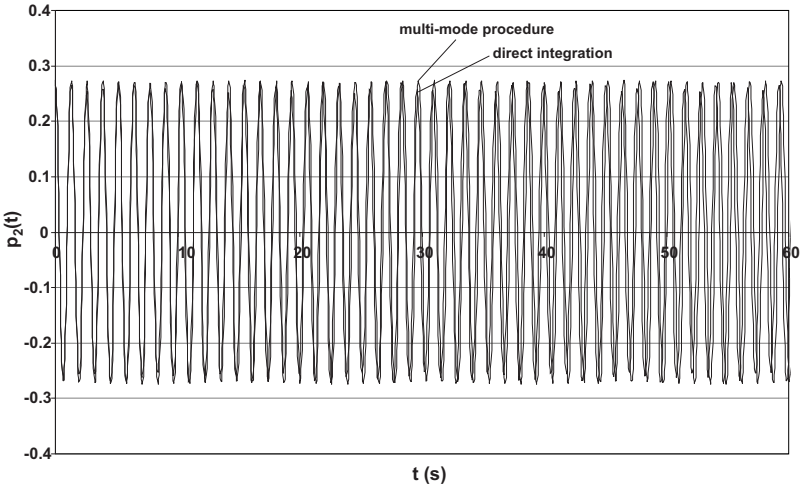

Fig. 11. Time-response for $p_2(t)$ co-ordinate.

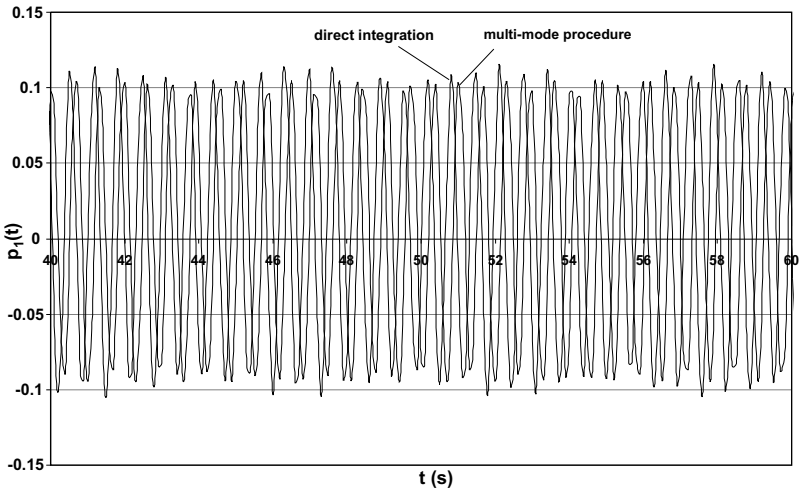

Fig. 12. Time-response for $p_1(t)$ co-ordinate.

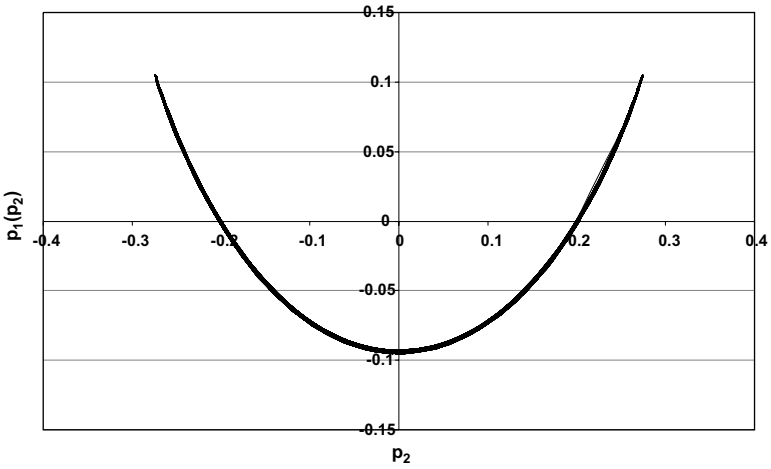

Fig. 13. Phase-trajectory projection onto the $p_1 \times p_2$ phase plane.

Here, shifts between the numerical and analytical results are small for the earlier times, but grow considerably as t increases.

Another interesting way to recognize the quasi-stationary state of this particular simulation is to inspect the projections of phase trajectories—embedded on the four-dimensional invariant manifold—onto the $p_1 \times p_2$ phase plane, as seen in Fig. 13.

6. Example 3: portal frame

The third selected example of multi-mode evaluation is the extremely slender portal frame indicated in Fig. 14. It was discretised with 14 Bernoulli–Euler non-linear finite-elements—see Mazzilli (1990) and Brasil and Mazzilli (1993)—, comprising 39 degrees of freedom, as seen in Fig. 15.

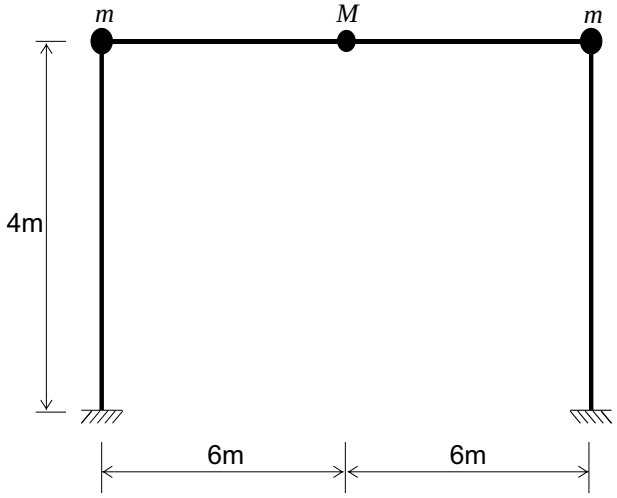

Fig. 14. Portal frame with distributed and lumped masses.

Both columns (length $h = 4$ m) and beam (length $\ell = 12$ m) are made of $4'' \times 4''$ H-type steel rods, for which the following data apply: Young's modulus $E = 2.05 \times 10^{11}$ N/m^2, mass per unit length $\tilde{m} = 20.5$ kg/m, cross section area $A = 2.61 \times 10^{-3}$ m^2, moment of inertia $I = 4.45 \times 10^{-6}$ m^4. The acceleration of gravity was taken as $g = 9.81$ m/s^2. Lumped masses, as shown in Fig. 15, $m = 3372$ kg and $M = 878$ kg, are purposefully large to introduce relevant geometric non-linearity into the analysis. In fact, the large axial force in the columns degrades the frame stiffness, so that the relevant natural frequencies noticeably decrease. Further, due to the beam large displacements, the deformed equilibrium configuration cannot be ignored in the analysis. Altogether, this is a remarkably defying example.

It is seen that such a system is internally resonant, when free-vibrations about the deformed equilibrium configuration take place. In fact, the frequencies of the first two modes are approximately in the 1:2 ratio,

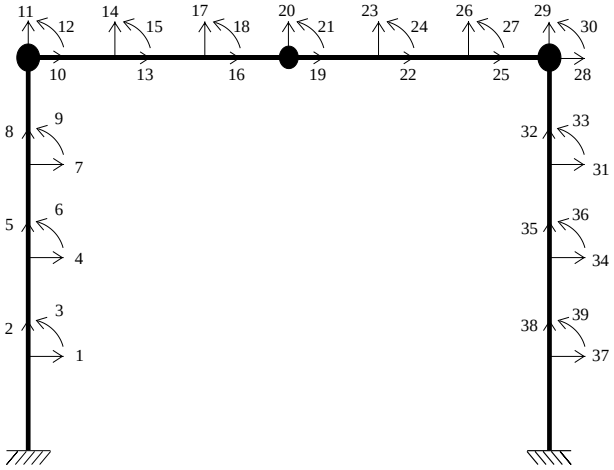

Fig. 15. Finite-element model for portal frame.

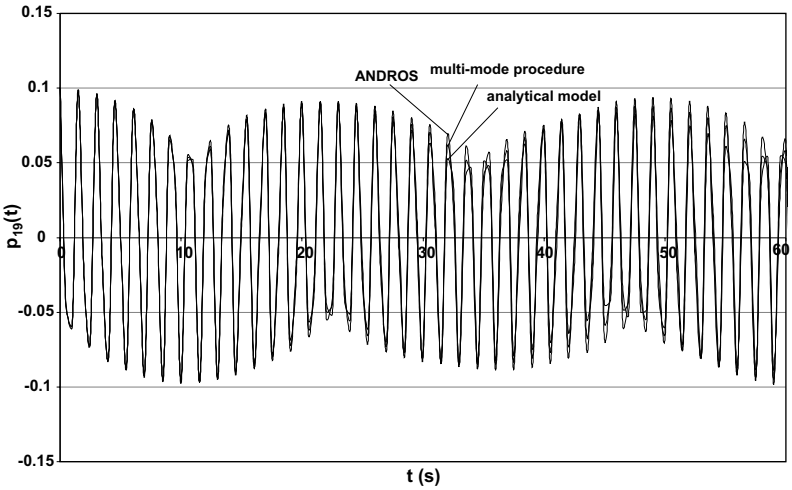

Fig. 16. Time-response for $U_1 = p_{19}(t)$ modal co-ordinate.

i.e. the first symmetric mode frequency (8.13 rd/s) is nearly twice that of the first anti-symmetric or sway mode (4.09 rd/s), as evaluated from the eigenvalue problem in terms of the tangent stiffness matrix. Should the eigenvalue problem be solved for the vibrations about the undeformed configuration, the frequencies would be 8.60 rd/s and 4.45 rd/s, respectively, and the internal resonance de-tuning would appear much larger.

To obtain the deformed equilibrium configuration for the finite-element model, which is an input for the multi-mode evaluation, it was used the ANDROS program—see Mazzilli and Brasil (1992)—, based on the same formulation.

The modal variables chosen were the horizontal displacement at mid span ($U_1 = p_{19}$) and its velocity ($V_1 = \dot{p}_{19}$), for the sway mode, and the vertical displacement at mid span ($U_2 = p_{20}$) and its velocity ($V_2 = \dot{p}_{20}$), for the first symmetric mode.

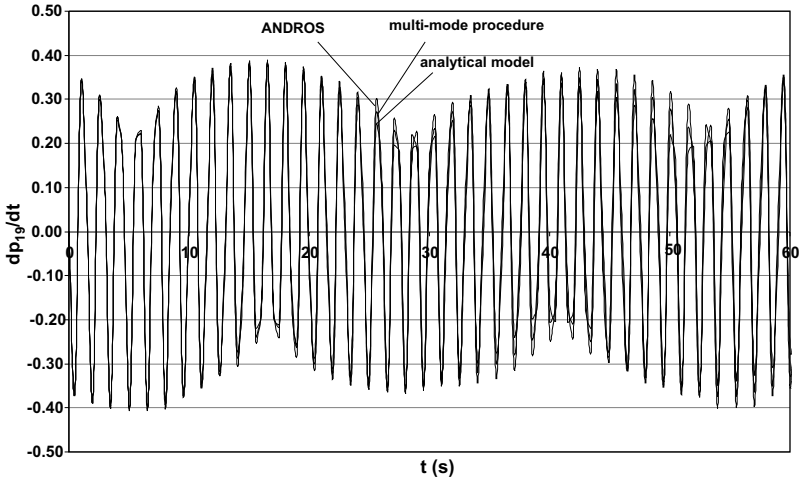

Fig. 17. Time-response for $V_1 = \dot{p}_{19}(t)$ modal co-ordinate.

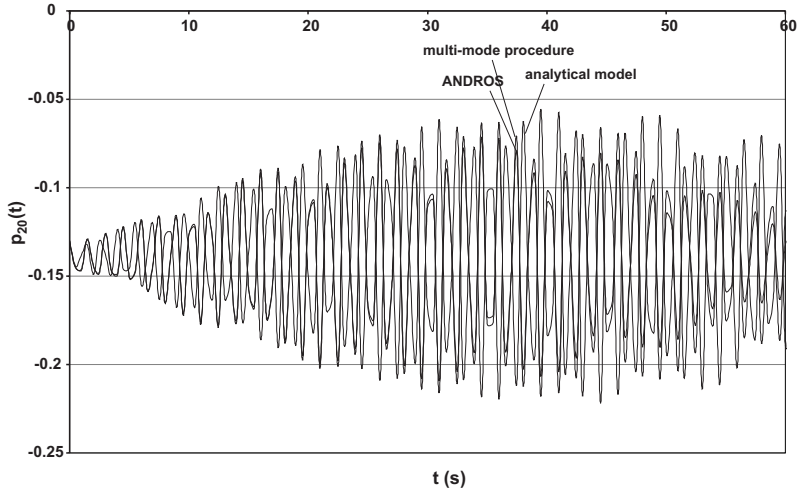

Fig. 18. Time-response for $U_2 = p_{20}(t)$ modal co-ordinate.

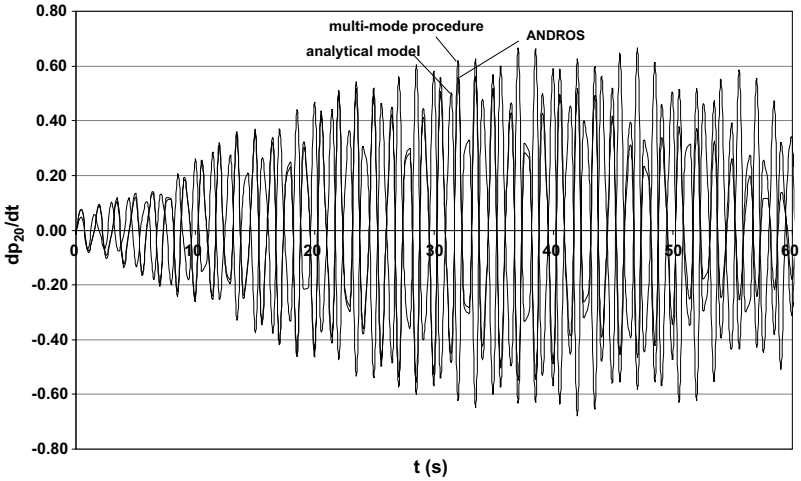

Fig. 19. Time-response for $V_2 = \dot{p}_{20}(t)$ modal co-ordinate.

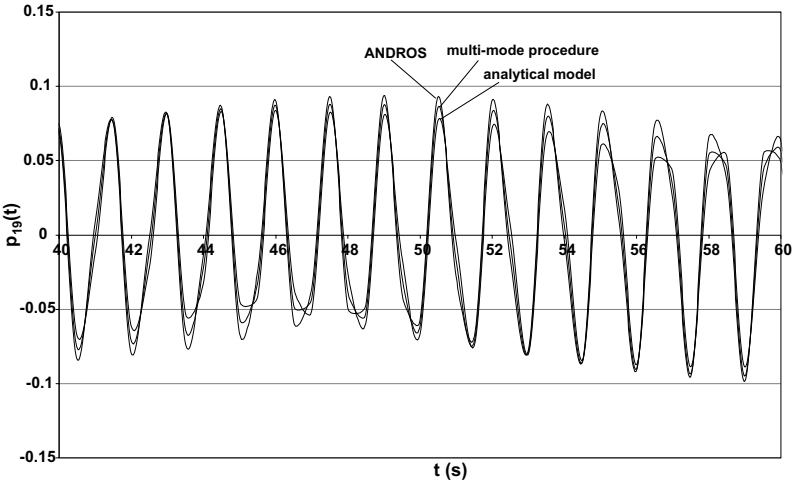

Fig. 20. Zooming of the time-response for $U_1 = p_{19}(t)$ modal co-ordinate.

Numerical and analytical solutions for this problem, considering a simplified two-degree-of-freedom model, were already addressed in Mazzilli and Brasil (1995), under a different viewpoint than that of the multi-mode evaluation.

In Figs. 16–19, the time responses for the modal variables are displayed, as they come out from the technique proposed herewith, from the ANDROS program and also from the numerical integration of the equations of motion proposed in Mazzilli and Brasil (1995).

The time-responses of Figs. 16–19 reveal a complex non-linear vibration pattern. Comparison of results is best seen zooming those graphs, say from $t = 40$ s to $t = 60$ s. For $U_1 = p_{19}$, the multi-mode results agree very well with those from ANDROS and from the two-degree-of-freedom system, as seen in Fig. 20.

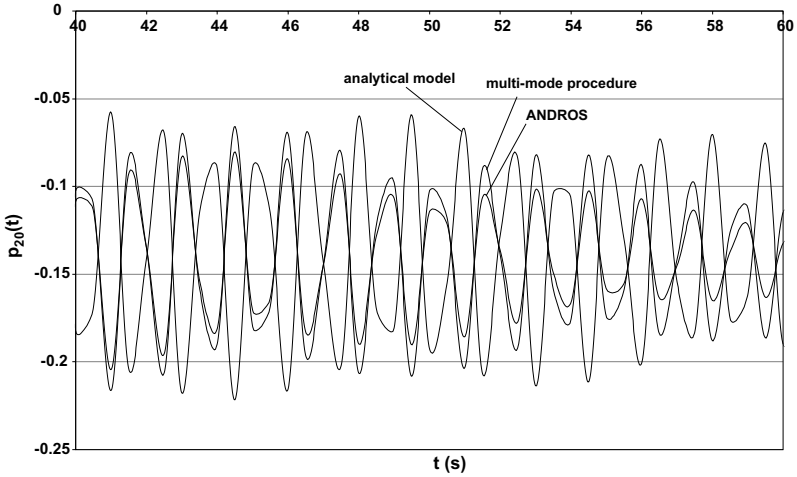

Fig. 21. Zooming of the time-response for $U_2 = p_{20}(t)$ modal co-ordinate.

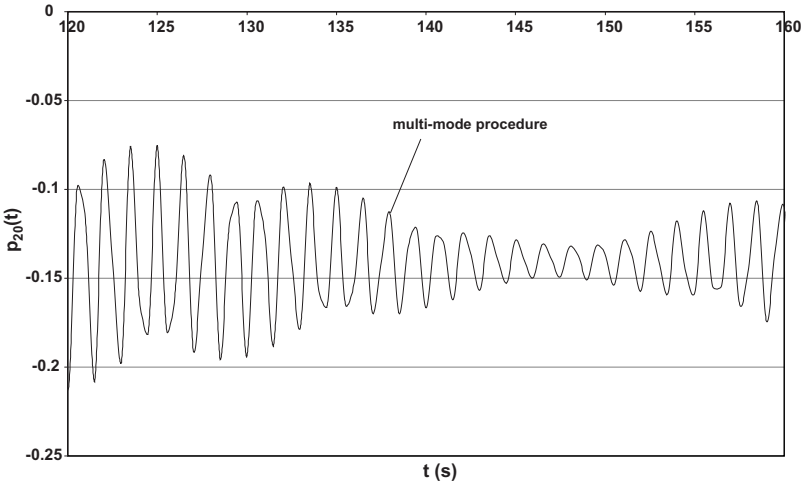

Fig. 22. Multi-mode time-response for $U_2 = p_{20}(t)$, 120 s $\leqslant t \leqslant$ 160 s.

For $U_2 = p_{20}$, agreement is not as good. For earlier times, the multi-mode results are still qualitatively close to those from ANDROS, although these latter ones are quantitatively smaller. Yet, the results from the two-degree-of-freedom system already display a phase shift with respect to those from both the multi-mode and ANDROS, not to mention larger amplitudes, as seen in Fig. 21. It is expected that the explanation for this might be related to the assumptions and simplifications made upon the displacement field for the two-degree-of-freedom system.

As time increases, due to small differences in the non-linear frequencies $\omega_i = \beta_i + \dot{\theta}_i$, the multi-mode and ANDROS curves also shift from one another, although still displaying the same pattern. For instance, what happens with the multi-mode results between $t = 120$ s and 160 s is approximately the same that happens with ANDROS results between $t = 100$ s and 140 s, as seen in Figs. 22 and 23. Here, it should be recalled

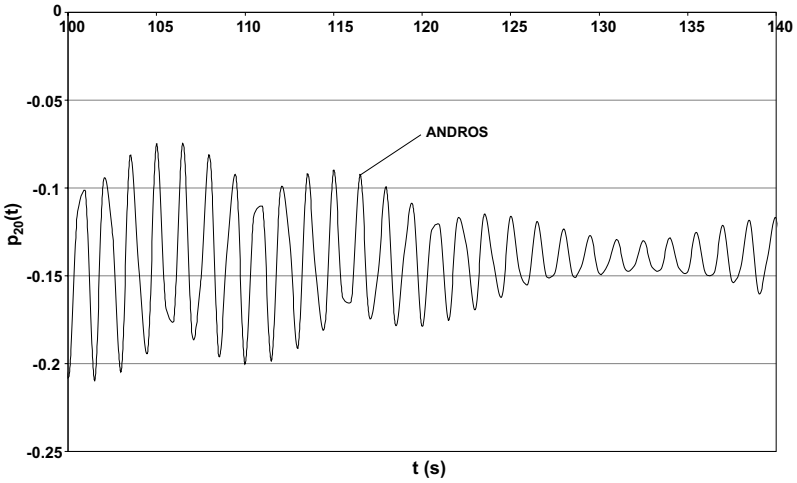

Fig. 23. ANDROS time-response for $U_2 = p_{20}(t)$, 100 s $\leqslant t \leqslant$ 140 s.

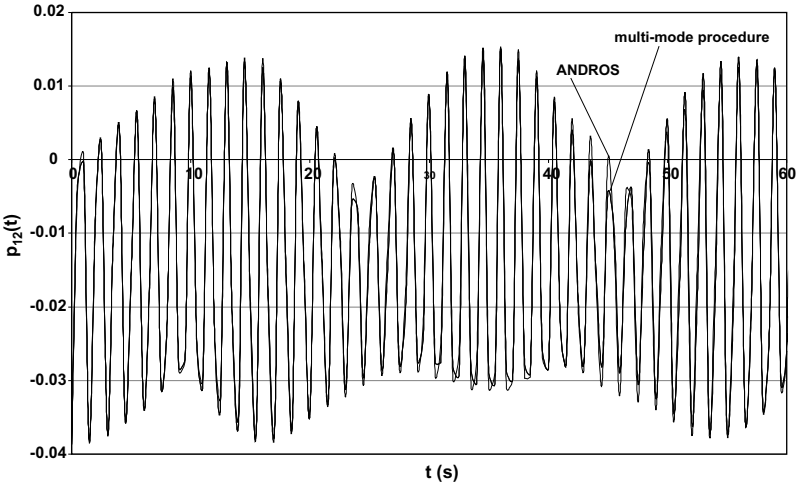

Fig. 24. Multi-mode and ANDROS time-responses for $p_{12}(t)$.

that the multi-mode expansions were truncated for terms of order larger than ε^2, whereas ANDROS takes into account up to cubic non-linearities.

To check the invariant manifold description of a generalised co-ordinate other than the modal variables, it was selected p_{12}, which stands for the beam left-end rotation. The results for $p_{12}(U_1, V_1, U_2, V_2)$, as in (42), agree perfectly with those of the time response (35) and those from ANDROS, as seen in Fig. 24.

The correlation between the multi-mode and ANDROS results for velocities is expected to be worse than for displacements, as already seen. Fig. 25 shows large deviations for $\dot{p}_{12}$, in spite of fine agreement for p_{12}.

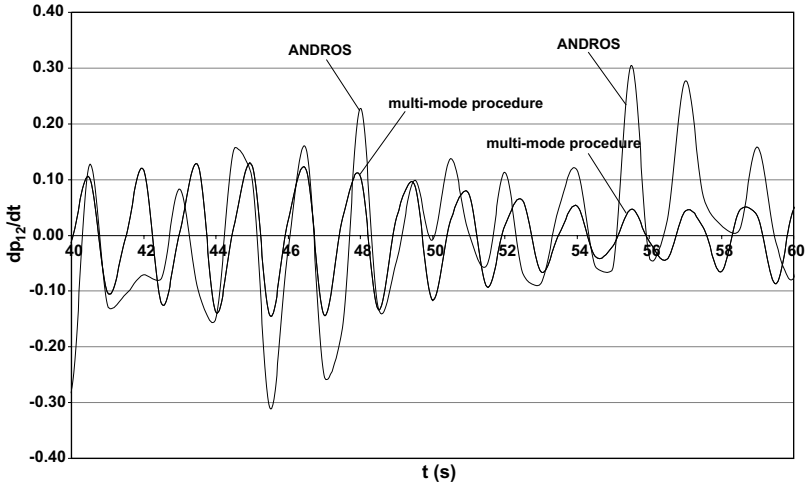

Fig. 25. Multi-mode and ANDROS time-responses for $\dot{p}_{12}(t)$.

7. Concluding remarks

The paper addresses the challenging issue of evaluation of non-linear multi-modes for finite-element models, using the method of multiple scales. The formulation presented herewith was implemented in symbolic mathematics and is capable of handling problems of several tens of degrees of freedom in a PC platform. Substitution of symbolic implementation by faster numerical codes, together with parallel computing may not only speed up the analyses, but also allow to tackle much larger problems. Pursuing further the asymptotic expansions up to terms of order ε^3 may lead to even better results, although the essential characteristics of multi-modes in the case of 1:2 internal resonance have already been captured.

Acknowledgement

The authors acknowledge the support to their research project provided by CNPq, Conselho Nacional de Desenvolvimento Científico e Tecnológico, under the grants 143001 and 304286.

References

Baracho Neto, O.G.P., 2003. Normal modes and multi-modes in the dynamics of structures with non-linear behaviour (in Portuguese), Ph.D. Thesis, Escola Politécnica, University of São Paulo, Brasil.

Baracho Neto, O.G.P., Mazzilli, C.E.N., 2005. Evaluation of multi-modes for finite-element models: systems tuned into 1:3 internal resonance. Journal of Sound and Vibration, to be submitted.

Boivin, N., Pierre, C., Shaw, S.W., 1994. Non-linear modal analysis of structural systems using multi-mode invariant manifolds, AIAA Dynamics Specialists Conference, South Carolina, AIAA Paper 1672, unrevised version.

Boivin, N., Pierre, C., Shaw, S.W., 1995a. Nonlinear normal modes, invariance and modal dynamics approximations of nonlinear systems. Nonlinear Dynamics 8, 315–346.

Boivin, N., Pierre, C., Shaw, S.W., 1995b. Non-linear modal analysis of structural systems featuring internal resonances. Journal of Sound and Vibration 182 (2), 336–341.

Brasil, R.M.L.R.F., Mazzilli, C.E.N., 1993. A general formulation of nonlinear dynamics applied to accessing the statical loading effect upon the dynamic response of planar frames. Applied Mechanics Review 46 (11), 110–117.

Mazzilli, C.E.N., 1982. A class of non-linear vibrations and their stability, Tese de Doutorado, University College, London.

Mazzilli, C.E.N., 1990. Non-linear finite-element formulation in dynamics II, ISSN 0103-9822, BT/PEF-9008, Boletim Técnico do Departamento de Engenharia de Estruturas e Fundações, Escola Politécnica, University of São Paulo.

Mazzilli, C.E.N., Brasil, R. M. L. R. F., 1992. ANDROS—A finite-element program for nonlinear dynamics, ISSN 0103-9822, BT/PEF-9213, Boletim Técnico do Departamento de Engenharia de Estruturas e Fundações, Escola Politécnica, University of São Paulo.

Mazzilli, C.E.N., Brasil, R.M.L.R.F., 1995. Effects of static loading on the nonlinear vibrations of a three-time redundant portal frame: analytical and numerical studies. Nonlinear Dynamics 8, 347–366.

Mazzilli, C.E.N., Soares, M.E.S., Baracho Neto, O.G.P., 2001. Reduction of finite-element models of planar frames using non-linear normal modes. International Journal of Solids and Structures 38, 1993–2008.

Mazzilli, C.E.N., Baracho Neto, O.G.P., 2002. Evaluation of non-linear normal modes for finite-element models. Computers and Structures 80, 957–965.